COMMUNICATIONS

Synthesis and Characterization of a Head–Tail Type Polycation Block Copolymer as a Nonviral Gene Vector

Atsushi Harada,* Masanori Kawamura, Takashi Matsuo, Toshinari Takahashi, and Kenji Kono

Department of Applied Chemistry, Graduate School of Engineering, Osaka Prefecture University, 1-1 Gakuen-cho, Sakai, Osaka 599-8531, Japan . Received September 29, 2005; Revised Manuscript Received December 5, 2005

A head–tail type polycation block copolymer, which is composed of the polyamidoamine (PAMAM) dendron and poly(L-lysine) (PLL) blocks, was newly designed as a nonviral gene vector in this study. This block copolymer (PAMAM dendron-PLL) was successfully synthesized in two steps: the synthesis of the PAMAM dendron block and the polymerization of the PLL block from the PAMAM dendron block. PAMAM dendron and PLL blocks in block copolymer showed independent deprotonation behavior, and their pK_a were determined to be 6.8 and 9.0, respectively. The complexation with pDNA was evaluated by gel retardation assay and dye exclusion assay, and both assays indicated that pDNA was selectively complexed with PLL block of block copolymer. Also, the PAMAM dendron-PLL poplyplexes showed 10^2 fold higher transfection efficiency to HeLa cells as that for PLL polyplexes. This might be due to the buffering effect of the PAMAM dendron block. This block copolymer could produce a function share in each block, i.e., tail block complexed with pDNA and head block showed a buffering effect. This molecular design of the head–tail type block copolymer might provide a new approach for realizing in vivo gene therapy.

The delivery of nucleic acids to cells as well as the instability in blood are important subjects for successful in vivo gene therapies. The design of synthetic polycation as nonviral gene vectors has received considerable attention for the purpose of realizing in vivo gene therapy (*1*–*4*). Although numerous polycations have been designed and synthesized, the rational design of polymers as in vivo gene vector systems has not yet been established. The use of polycations with relatively low pK_a values are mentioned as one of the guidelines. Polycations with low pK_a values, such as polyethyleneimine (PEI) and polyamidoamine (PAMAM) dendrimer, exhibit a high transfection efficiency due to the buffering effect (*5*–*8*), and PEI and PAMAM dendrimer are marketed under the trade names of ExGene and SuperFect, respectively. However, these have relatively weak affinity to DNA compared with cationic polymers, such as poly(L-lysine) (PLL) having a high pK_a value. One looks forward to the design of polycations, which combines stable complex formation under physiological conditions and a buffering effect. Recently, Kataoka et al. reported the polyplex vectors from A–B–C type triblock copolymers with spatially ordered layering of the condensed pDNA and buffering units for enhanced intracellular gene delivery (*9*). Such a molecular design, which produces a function share in each block of the copolymer, could be effective in realizing in vivo gene therapy. Here, we have newly designed a head–tail type polycation block copolymer, which is composed of the PAMAM dendron as the head block and PLL as the tail block, as a nonviral gene vector (Figure 1). In the design of the block copolymer composed of polycation blocks with different pK_a values as the gene vector, it is important that the pK_a values of the polycation block with a relatively low pK_a value be maintained even after the block copolymerization with different kind of polycations as well as the complexation with the pDNA. Consequently, the PAMAM dendron was selected as a buffering block with a low pK_a value, since the tertiary amino groups in the interior of the PAMAM dendron cannot be easily influenced by another polycation block due to steric hindrance. It was expected that the head and tail blocks exhibit a buffering action and complexation with pDNA, respectively.

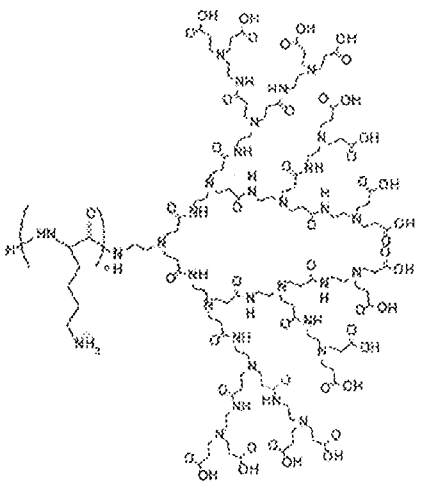

Figure 1. The chemical structure of head–tail type polycation block copolymer.

The head–tail type polycation block copolymer was synthesized in two steps, i.e., the synthesis of the PAMAM dendron

* To whom correspondence should be addressed. Tel and Fax: +81-72-254-9328, e-mail: harada@chem.osakafu-u.ac.jp.

10.1021/bc0502863 CCC: $33.50
Published on Web 12/22/2005

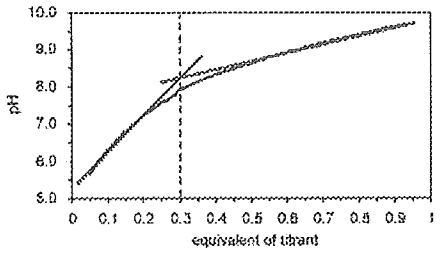

Figure 2. Titration curve of PAMAM dendron-PLL. 150 mg of PAMAM dendron-PLL in 45 mL of 0.01 M HCl was titrated with 0.01 M NaOH. The titrant was added in 0.1 mL quantities at 25 °C.

block and the polymerization of the PLL block from the PAMAM dendron block. Briefly, the PAMAM dendron block was synthesized by the repetitive exhaustive Michael addition with methyl acrylate using *tert*-butyl *N*-(2-aminoethyl)carbamate], for which one amino group of ethylenediamine is protected by a *tert*-butoxycarbonyl (Boc) group, as the starting reagent and subsequent exhaustive amidation with ethylenediamine (*10*). With four repetitions of the Michael addition and three amidations, the PAMAM dendron (Boc-PAMAM dendron) was made. To polymerize the PLL block from the PAMAM block, the Boc group at the root of the PAMAM dendron was removed by CF_3COOH treatment. The polymerization of the ϵ-benzyloxycarbonyl L-lysine *N*-carboxy anhydride [Lys(Z)-NCA], which was synthesized by the Fuchs−Farthing method using triphosgene (*11*), was then initiated from the primary amino group at the root of the PAMAM dendron in DMF at 40 °C. The obtained PAMAM dendron-PLL(Z) was converted to the PAMAM dendron-PLL by acid treatment using 30% HBr/AcOH in TFA. Also, the peripherial group of the PAMAM dendron block (methyl ester group) was removed by alkali treatment and converted to a carboxylate group. The finally obtained PAMAM dendron-PLL had 16 carboxylate groups at the periphery of the head block, 15 tertiary amino groups in the interior of the head block, and 70 primary amino groups in the tail block.

The deprotonation behavior of the PAMAMA dendron-PLL was important for determining the properties as a gene vector. The change in the ionization state vs the pH change was evaluated by an acid−base titration. Figure 2 shows the acid−base titration curve, pH vs equivalent of titrant, of the PAMAMA dendron-PLL. Obviously, two independent deprotonation processes were observed bound at equivalents of titrant = 0.3. The deprotonation at equivalents of titrant < 0.3 was due to the deprotonation of the tertiary amino groups in the interior of the PAMAM dendron block and carboxylate groups at the periphery of the PAMAM dendron block, and the deprotonation at equivalents of titrant > 0.3 was due to the primary amino groups of the PLL block. This might be a reasonable quantity for deprotonation, since the numbers of ionizable groups were 70 for the PLL block and 31 for the PAMAM dendron block. The pK_a values for each block were 9.0 for the PLL block and 6.8 for the PAMAM dendron block. Such a property vs the pH change (independent deprotonation behavior) as shown in Figure 2 was quite important in the design of the polycation block copolymer which makes a function share in each block. In the case of the design of polyelectrolytes having different kinds of weakly ionizable groups with different pK_a values, it is difficult to maintain the pK_a values for each ionizable group, because the pK_a value of a weakly ionizable group is shifted by the effect of the neighboring groups (*12*). Also, by pH change from physiological pH (7.4) to endsomal pH (less than 6.0), equivalents of titrant changed from 0.23 to 0.08. This suggests that the PAMAM dendron block exhibits a proton sponge nature in the uptake process into the cells.

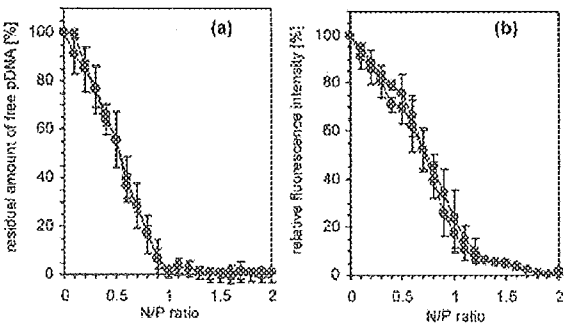

Figure 3. Complexation of pDNA with PAMAM dendron-PLL (red) and PLL (blue) evaluated by gel retardation assay (a) and dye exclusion assay (b). In part a, the gel electrophoresis was carried out at 100 V/cm for 30 min with 0.6 w/w% agarose gel, and residual amounts of free pDNA was determined by analyzing the magnitude of ethidium bromide-stained bands for free pDNA. In part b, fluorescence intensities for the polyplex solutions containing 10 μg of pDNA/mL and 2.5 μg of ethidium bromide (EtBr)/mL were measured. The excitation and emission wavelengths were 510 and 590 nm, respectively. For both experiments, the N/P ratio was defined as the number of ϵ-amino groups of PLL vs the number of phosphate groups of pDNA, and the data are presented as the average of three experiments ± SD.

The polyplex solutions were prepared by mixing pDNA and polycation solutions, after pDNA and polycations, PAMAM dendron-PLL or PLL, were separately dissolved in 20 mM Tris-HCl buffer (pH 7.4). The complexation of the PAMAM dendron-PLL with pDNA was evaluated by two assays, i.e., the dye exclusion assay and gel retardation assay (Figure 3). For both assays, the PAMAM dendron-PLL and PLL showed identical profiles with the change in the N/P ratios, in which the N/P ratio was defined as the number of ϵ-amino groups of PLL vs the number of phosphate groups of pDNA, nevertheless, the PAMAM dendron-PLL has tertiary amino groups in the PAMAM dendron block. Also, the addition of the Boc-PAMAM dendron to pDNA did not induce any complexation, since the tertiary amino groups in the interior was not protonated at pH 7.4. The protonation of the tertiary amino groups in the PAMAM dendron block was not facilitated by the complexation with pDNA via electrostatic interactions between pDNA and PLL. It was expected that the tertiary amino groups of the PAMAM dendron block in the PAMAM dendron-PLL might show a buffering effect.

From the transfection efficiency toward the culture cells (HeLa cells), it was indirectly evaluated whether the PAMAM dendron-PLL vector exhibits the buffering effect. It was known that the polyplexes of pDNA with the PLL homopolymer required the use of a lysosomotropic reagent such as chloroquine in order to express a sufficient transfection efficiency. Indeed, the PLL polyplexes showed a very low transfection efficiency to HeLa cells in the absence of the lysosomotropic reagent (Figure 4). On the other hand, the PAMAM dendron-PLL system showed a considerably high transfection efficiency compared with the PLL polyplex. Comparing the transfection efficiency at N/P = 3.5, at which PAMAM dendron-PLL polyplexes showed highest transfection efficiency, PAMAM dendron-PLL polyplexes showed 10^2 times as high transfection efficiency as PLL polyplexes, suggesting a buffering effect during endosomal/lysosomal processes. Also, when pDNA was complexed with the mixture of PLL and the Boc-PAMAM dendron, the complexes did not exhibit a sufficient transfection efficiency, and there was no difference with as significant their transfection efficiency as transfection efficiency of PLL polyplexes in the evaluated N/P ratio range. That is, the block copolymerization with the PAMAM dendron was required for expressing the buffering effect. Further, it should be noted the

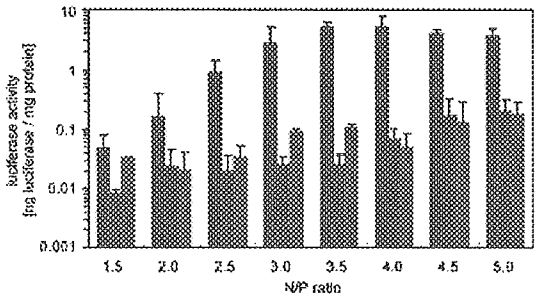

Figure 4. Transfection efficiency of PAMAM dendron-PLL polyplexes (red), PLL polyplexes (blue), and the mixture of PAMAM dendron and PLL (green) to HeLa cells. The cells (5×10^4) were treated with the polyplexes including 1 μg of pDNA. The N/P ratio was defined as the number of ϵ-amino groups of PLL vs the number of phosphate groups of pDNA. The data are presented as the average of three experiments ± SD.

difference in the effect of N/P ratio between the complexation (Figure 3) and transfection efficiency (Figure 4). The transfection efficiency of PAMAM dendron-PLL was increasing to N/P = 3.5, although both residual amounts of free pDNA and relative fluorescence intensity were almost no change at N/P > 1. This might worry the influence of free PAMAM dendron-PLL, i.e., uncomplexed PAMAM dendron-PLL, to an increase in transfection efficiency. To confirm the change in the property of polyplexes, the zeta-potential measurements were carried out for the PAMAM dendron-PLL polyplexes prepared at varying N/P ratios. The zeta-potentials of the complexes of PAMAM dendron-PLL with pDNA changed in this N/P ratio range ($1 < N/P < 3.5$), and the zeta-potentials of pDNA/PAMAM dendron-PLL at N/P = 1.0, 1.5, 2.0 and 3.5 were −20.9±1.7, 9.1±0.7, 15.8±0.9 and 24.7±2.4 mV, respectively. This indicates that the properties of pDNA/PAMAM dendron-PLL changed with an increase in N/P ratio even at $1.0 < N/P < 3.5$. Consequently, the increase in transfection efficiency at $1.5 < N/P < 3.5$ shown in Figure 4 might be induced by the effect of increasing the relative number of PAMAM dendron block, which exhibit a buffering effect, against pDNA and the effect of the change in the complex properties including zeta-potentials.

In conclusion, a head−tail type polycation block copolymer, which is composed of a PAMAM dendron as the head block and PLL as the tail block, was newly designed as a nonviral gene vector. The head−tail type block copolymer complexed with pDNA is driven by electrostatic interactions between pDNA and PLL block. Also, the polyplexes of the head−tail type block copolymer showed a sufficient transfection efficiency due to the buffering effect of the PAMAM dendron block even in the absence of a lysosomotropic reagent. This molecular design of the head−tail type block copolymer might provide a new approach to the realization of in vivo gene therapy.

ACKNOWLEDGMENT

This work was financially supported by a Grant-in-aid for Scientific Research form the Ministry of Education, Science, Sports, and Culture in Japan.

Supporting Information Available: The detailed procedure and characterization of block copolymer synthesis and the experimental procedure of dye exclusion assay, gel retardation assay, the transfection to HeLa cells, and zeta-potential measurements. This material is available free of charge via the Internet at http://pubs.acs.org.

LITERATURE CITED

(1) Felgner, P. L. (1990) Particulate systems and polymers for in vitro and in vivo delivery of polynucleotides. *Adv. Drug Delivery Rev. 5*, 163−187.

(2) Behr, J. P. (1994) Gene transfer with synthetic cationic amphiphiles: Prospects for gene therapy. *Bioconjugate Chem. 5*, 382−389.

(3) Kabanov, A. V., and Kabanov, V. A. (1995) DNA complexes with polycations for the delivery of geneticmaterial into cells. *Bioconjugate Chem. 6*, 7−20.

(4) Stull, R. A., and Szoka, F. (1995) Antigen, ribozyme and aptamer nucleic-acid drugs − progress and prospects. *Pharm. Res. 12*, 465−483.

(5) Boussif, O., Lezoualæh, F., Zanta, M. A., Mergny, M. D., Scherman, D., Demeneix, B., and Behr, J. P. (1995) A versatile vector for gene and oligonucleotide transfer into cells in culture and in-vivo − polyethyleneimine. *Proc. Natl. Acad. Sci. U.S.A. 92*, 7297−7301.

(6) Behr, J. P. (1997) The proton sponge: A trick to enter cells the viruses did not exploit. *Chemia 51*, 34−36.

(7) Tang, M., Redemann, C. T., and Szoka, F. C. Jr. (1996) In vitro gene delivery by degraded polyamidoamine dendrimers. *Bioconjugate Chem. 7*, 703−714.

(8) Kukowska-Latallo, J. F., Bielinska, A. U., Johnson, J., Spindler, R., Tomalia, D. A., and Baker, J. R., Jr. (1996) Efficient transfer of genetic material into mammalian cells using starburst polyamidoamine dendrimers. *Proc. Natl. Acad. Sci. U.S.A. 93*, 4897−4902.

(9) Fukushima, S., Miyata, K., Nishiyama, N., Kanayama, N., Yamasaki, Y., and Kataoka, K. (2005) PEGylated polyplex micelles from triblock cationers with spatially ordered layering of condensed pDNA and buffering units for enhanced intracellular gene delivery. *J. Am. Chem. Soc. 127*, 2810−2811.

(10) Tomalia, D. A., Baker, H., Dewald, J., Hall, M., Kallos, G., Martin, S., Roeck, J., Ryder, J., and Smith, P. (1985) A new class of polymers − starburst-dendritic macromolecules. *Polym. J. 17*, 117−132.

(11) Harada, A., and Kataoka, K. (1995) Formation of polyion complex micelles in an aqueous milieu from a pair of oppositely charged block copolymers with poly(ethylene glycol) segments. *Macromolecules 28*, 5294−5299.

(12) Morawetz, H. *Macromolecules in solution*; Interscience Publishers, New York, 1985.

BC0502863

Temperature Sensitization of Liposomes by Use of Thermosensitive Block Copolymers Synthesized by Living Cationic Polymerization: Effect of Copolymer Chain Length

Kenji Kono,*,† Taishi Murakami,† Tomohide Yoshida,‡ Yasuhiro Haba,† Shokyoku Kanaoka,‡ Toru Takagishi,† and Sadahito Aoshima‡

Department of Applied Chemistry, Graduate School of Engineering, Osaka Prefecture University, 1-1, Gakuen-cho, Sakai, Osaka 599-8531, Japan, and Department of Macromolecular Science, Graduate School of Science, Osaka University, Toyonaka, Osaka 560-0043, Japan. Received January 10, 2005; Revised Manuscript Received September 25, 2005

We prepared block copolymers of (2-ethoxy)ethoxyethyl vinyl ether (EOEOVE) and octadecyl vinyl ether (ODVE) with the number average molecular weights of 6900, 9300, and 16 700 by living cationic polymerization. The poly(EOEOVE) block acts as a temperature-sensitive moiety, and the poly(ODVE) block acts as an anchor moiety. We also investigated the effect of chain length of the copolymer poly(EOEOVE) block on the ability to sensitize liposomes. The copolymers underwent a coil−globule transition at ~36 °C in the presence of a membrane of egg yolk phosphatidylcholine (EYPC), detected using differential scanning calorimetry (DSC). Liposomes encapsulating calcein, a water-soluble fluorescent dye, were prepared from mixtures of dioleoylphosphatidylethanolamine, EYPC, and the copolymers. While the copolymer-modified liposomes released little calcein below 30 °C, release was enhanced above 35 °C, indicating that dehydrated copolymer chains destabilized the liposome membrane. In addition, copolymers with a longer poly(EOEOVE) block induced a more drastic enhancement of contents release in a narrow temperature region near the transition temperature of the poly(EOEOVE) block. As a result, the copolymer with an average molecular weight of 16 700 generated highly sensitive liposomes that produced rapid and dramatic release of the contents in response to temperature.

1. INTRODUCTION

Liposomes are highly attractive materials for drug delivery because of their biocompatibility, ability to encapsulate both hydrophilic and hydrophobic drugs, and size controllability (*1*). Therefore, studies to modify their functions have been conducted to increase their usefulness. While various functional liposomes have been developed, temperature-sensitive liposomes have received much attention (*2*−*4*). Temperature-sensitive liposomes have been produced by modifying liposomes with thermosensitive polymers according to methods by Kono et al. (*5*, *6*) and other groups (*7*−*10*).

The water solubility and conformation of thermosensitive polymers change at a specific temperature, called the lower critical solution temperature (LCST). These changes in water solubility and conformation provide temperature-sensitive properties to liposomes (*6*). Poly(*N*-isopropylacrylamide) [poly(NIPAM)] and copolymers of NIPAM, prepared via free radical polymerization, have been used for temperature-sensitization of liposomes (*5*−*7*, *9*, *11*−*13*). Highly hydrated polymer chains conjugated to the liposome surface increase the stability of liposomes below the LCST (*13*, *14*). In contrast, above the LCST, dehydrated polymer chains interact with the liposome membrane and induce release of the liposome contents (*6*). However, polymers and copolymers produced by this technique can have disadvantages, such as lack of control over molecular weight, high polydispersity, and limited freedom in choosing the architecture of the polymer chain, although efforts have been made recently to synthesize homopolymer and block copolymers of NIPAM with a defined structure by atom transfer polymerization (*15*) or reversible addition−fragmentation chain transfer polymerization (*16*−*18*).

Living cationic polymerization is an attractive technique for the synthesis of thermosensitive polymers with precisely controlled molecular architecture and molecular weight. In fact, a variety of thermosensitive polymers and block copolymers with controlled molecular structures have been prepared using this polymerization system (*19*−*21*). Aoshima et al. have shown that living cationic polymerization of 2-(2-ethoxy)ethoxyethyl vinyl ether (EOEOVE) gives a thermosensitive polymer, which allows control of molecular weight and a low polydispersity (*19*).

In this study, synthesis of block copolymers of EOEOVE and octadecyl vinyl ether (ODVE) for the sensitization of liposomes was examined (Figure 1). The poly(EOEOVE) block behaves as a thermosensitive moiety, whereas the poly(ODVE) block acts as an anchor for fixing the copolymer chain onto a liposomal membrane through hydrophobic interaction between its octadecyl chains and the liposome membrane. Temperature-sensitive content release or related behaviors were investigated for liposomes modified with the block copolymers having a poly(EOEOVE) block of varying chain lengths. The effect of chain length of the thermosensitive block

* To whom correspondence should be addressed. Phone: +81-72-254-9330. Fax: +81-72-254-9330. E-mail: kono@chem.osakafu-u.ac.jp.
† Osaka Prefecture University.
‡ Osaka University.

10.1021/bc050004z CCC: $30.25
Published on Web 11/01/2005

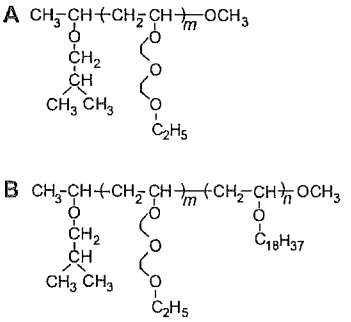

Figure 1. Structures of poly(EOEOVE) (A) and copoly(EOEOVE-*b*-ODVE) (B).

on the ability of block copolymers to sensitize liposomes is described.

2. EXPERIMENTAL SECTION

2.1. Materials. Egg yolk phosphatidylcholine (EYPC) and dioleoylphosphatidylethanolamine (DOPE) were kindly donated by Nippon Oil and Fats Co. (Tokyo, Japan). Octadecyl vinyl ether (ODVE) was obtained from BASF (Germany). 2-(2-Ethoxy)ethoxyethyl vinyl ether (EOEOVE) was purchased from Maruzen Petrochemical (Tokyo, Japan). Calcein, pyrenecarboxaldehyde (PyCHO) 1,6-diphenyl-1,3,5-hexatriene (DPH), and 8-anilino-1-naphthalenesulfonic acid (ANS) were obtained from Sigma-Aldrich Japan (Tokyo, Japan). $Et_{1.5}AlCl_{1.5}$ (1.0 M solution in toluene) and toluene were obtained from Wako Pure Chemical Industries (Osaka, Japan). Ethyl acetate was supplied from Nacalai Tesque (Kyoto, Japan). ODVE was distilled over calcium hydride under reduced pressure (150 °C/3 mmHg). EOEOVE was washed with 10% aqueous sodium hydroxide and then with water, dried overnight over potassium hydroxide pellets, and distilled twice over metallic sodium before use. Ethyl acetate was distilled at least twice over calcium hydride. Toluene as a polymerization solvent was washed by the usual method and distilled at least twice over calcium hydride and then metallic sodium just before use. Cationogen, 1-isobutylethyl acetate (IBEA) ($CH_3CH(OiBu)OCOCH_3$), was prepared from isobutyl vinyl ether (IBVE) and acetic acid and was distilled over calcium hydride under reduced pressure (*22*). All monomers, the $Et_{1.5}AlCl_{1.5}$ solution, and IBEA were stored in a brown ampule under dry nitrogen.

2.2. Polymerization Procedures. Polymerization was carried out at 0 °C under a dry nitrogen atmosphere in a glass tube equipped with a three-way stopcock baked at 240 °C for 10 min before use. The reaction was initiated by the addition of $Et_{1.5}AlCl_{1.5}$ solution in toluene into a mixture of a monomer, an added base, and the cationogen IBEA in toluene at 0 °C by a dry medical syringe. For block copolymerization, a typical example is as follows. EOEOVE (0.13 M, 0.11 mL) was first polymerized in the presence of $CH_3COOC_2H_5$ (1.0 M, 0.5 mL) as an added base ($[IBEA]_0$ = 4.0 mM; $[Et_{1.5}AlCl_{1.5}]_0$ = 20 mM in toluene). After 2.5 h, the second monomer, ODVE (0.04 M in toluene, 5.0 mL), was added to the reaction mixture at a given conversion of EOEOVE. After 2 h, ODVE had been consumed quantitatively (total 4.5 h). When the polymerization was finished, it was quenched with methanol containing a small amount of aqueous ammonia. The quenched reaction mixture was diluted with dichloromethane and then sequentially washed with dilute hydrochloric acid and with water to remove the initiator residues. The product polymer was recovered from the organic layer by evaporation of the solvent under reduced pressure and vacuum-dried overnight. Poly(NIPAM)s with different molecular weights were obtained by polymerization of NIPAM in tetrahydrofran using azobisisobutyronitrile as a free radical initiator as previously reported (*5*, *12*) and subsequent fractional precipitation by adding diethyl ether into poly(NIPAM) dissolved in tetrahydrofran.

2.3. Liposome Preparation. The liposomes were prepared as previously reported (*23*, *24*). A mixture of DOPE and EYPC (7:3, mol/mol) (4.4 mg) and varying amounts of the copolymer were dissolved in chloroform, and the solvent was removed by evaporation. The obtained thin lipid/copolymer-mixed membrane was further dried under vacuum overnight and dispersed in 0.75 mL of an aqueous calcein solution (63 mM, pH 7.4) or in 10 mM Tris-HCl-buffered solution containing 140 mM NaCl and 1 mM EDTA solution (pH 7.4). The obtained liposome suspension was extruded through a polycarbonate membrane with a pore diameter of 100 nm in an ice-cooled water bath. The free calcein and free copolymer were removed by gel permeation chromatography (GPC) on a Sepharose 4B column at 4 °C using a 10 mM Tris-HCl-buffered solution containing 140 mM NaCl and 1 mM EDTA solution (pH 7.4). The liposomes suspensions were kept at 5 °C until the measurements were made.

2.4. Calcein Release from Liposome. The release measurements were performed according to the method previously reported (*23*, *24*). An aliquot of dispersion of the calcein-loaded liposomes was added into 2 mL of 10 mM Tris-HCl, 140 mM NaCl, and 1 mM EDTA solution (pH 7.4) in a quartz cell (final concentration of the lipids, 10 μM) at a given temperature, and the fluorescence intensity of the solution was monitored using a spectrofluorometer (Shimadzu RF-5000). The excitation and monitoring wavelengths were 490 and 520 nm, respectively. The percent release of calcein from the liposomes was defined as

$$\% \text{ release} = \frac{F^t - F^i}{F^f - F^i} \times 100$$

where F^i and F^t mean the initial and intermediary fluorescence intensities of the liposome suspension, respectively. F^f is the fluorescent intensity of the liposome suspension after the addition of Triton X-100 (final concentration of 0.15%).

2.5. Estimation of the Amount of Copolymer Bound to Liposome. The amount of the copolymer bound to the liposome was estimated using high-performance liquid chromatography as previously reported (*12*, *13*). The liposomes bearing the copolymer were dried under vacuum and then dissolved in methanol/water (7:3, v/v). The solution was filtered through a poly(tetrafluoroethylene) membrane with a pore size of 0.25 μm. The filtrate (20 μL) was injected into a KB-8501 column (Showa Denko), and the amount of the copolymer was evaluated using a refractive index detector (Jasco, RI-930). Also, the lipid amount was determined by the method of Bartlett (*25*).

2.6. Fluorescence Measurements. Emission spectra of PyCHO were obtained on a spectrofluorometer with excitation at 365.5 nm. Fluorescence polarization (P) of DPH and ANS was measured as reported previously (*26*). Fluorescence polarization of DPH and ANS was measured as reported previously (*24*, *27*). ANS and DPH were excited at 395 and 360 nm, respectively, and the fluorescence intensities of ANS and DPH were monitored at

467 and 428 nm, respectively. The P value was evaluated using

$$P = \frac{I_p - I_v}{I_p + I_v}$$

where I_p and I_v represent the intensities of parallel polarized fluorescence and vertically polarized fluorescence, respectively.

2.7. Retention of Fluorescein Isothiocyanate (FITC)−Dextran in Liposomes. The liposomes containing FITC−dextran was prepared by suspending a dry membrane of EYPC (10 mg) or a mixture (9 mg) of DOPE and EYPC (7/3, mol/mol) in a solution of FITC−dextran (6 mg) dissolved in 10 mM Tris-HCl and 140 mM NaCl solution (1.5 mL, pH 7.4) at varying temperatures for 30 min. Then, the liposomes were applied to a Sepharose 4B column to remove FITC−dextran released from the liposomes during the incubation. The percent of FITC−dextran remaining after the incubation was calculated from

$$\text{FITC−dextran remaining (\%)} = \frac{F^0 - F^t}{F^0} \times 100$$

where F^0 and F^t mean the fluorescence intensities of FITC-dextran-loaded liposomes per liposomal lipid before and after 30 min of incubation and subsequent GPC using a Sepharose 4B column, respectively. The excitation and monitoring wavelengths of FITC−dextran were 490 and 520 nm, respectively.

2.8. Other Methods. The molecular weight distribution of poly(EOEOVE) and poly(EOEOVE-*block*-ODVE) was measured by size exclusion chromatography (SEC) in chloroform at 40 °C on three polystyrene gel columns [TSK gel G-2000HXL (molecular range of 1×10^2 to 1×10^4 (PSt)), 3000HXL (6×10^3 to 6×10^4), and 4000HXL (1×10^4 to 4×10^5); 7.8 mm i.d. × 300 mm; flow rate, 1.0 mL/min] connected to a Tosoh DP-8020 dual pump and a RI-8020 refractive detector. The number-average molecular weight (M_n), the weight-average molecular weight (M_w), and the polydispersity index (M_w/M_n) were calculated from SEC curves on the basis of a polystyrene calibration. M_n and M_w of poly(NIPAM)s were determined using SEC on a system equipped with a Shodex KF-805L and KD-803 column (Showa Denko) with differential refractive index detection (Jasco, RI-930) using DMF as an eluent and poly(ethylene glycol) as the standard. ^{1}H NMR and ^{13}C NMR spectra were recorded on a JEOL JNM-EX270 (270 MHz). Differential scanning calorimetry (DSC) was performed with a DSC 120 microcalorimeter (Seiko Electronics). The size of liposomes was evaluated by dynamic light scattering using a Nicomp 380 ZLS instrument (Particle Sizing Systems).

3. RESULTS AND DISCUSSION

3.1. Characterization of Polymers and Copolymers. Three types of poly(EOEOVE) with different molecular weights were prepared by controlling the molar ratio of monomer EOEOVE to initiator IBEA for the polymerization (Figure 1). Polymerization at EOEOVE/IBEA (mol/mol) ratios of 32, 60, and 120 gave polymers with average molecular weights of 5300, 8300, and 15 800, respectively, within narrow molecular weight distributions (Table 1). The degree of polymerization for these polymers was estimated to be 33, 52, and 99, respectively. We also prepared three poly(EOEOVE)s with an oligo(ODVE) block, which acts as an anchor for fixing the polymer chain onto a liposomal membrane, through sequential living copolymerization of EOEOVE and ODVE (Table 1). When the poly(EOEOVE) segments of the block copolymers and homopolymers of EOEOVE were prepared at the same monomer/initiator ratio, they contained essentially the same number of EOEOVE units in the polymer and copolymer chains. In addition, these block copolymers contained approximately the same number of ODVE units (four or five) at the terminal moiety of the copolymer chain. We have already shown that two dodecyl groups fix chains of NIPAM copolymers stably onto liposome membranes (*23*, *24*). Therefore, highly hydrophobic octadecyl groups of the ODVE block at the terminal moiety of the copolymer should fix the copolymer chain onto the liposome surface tightly through hydrophobic interactions.

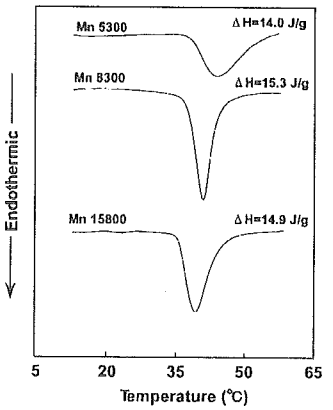

Figure 2. Microcalorimetric endotherms for poly(EOEOVE)s with M_n of 5300, 8300, and 15 800 in water.

Table 1. Preparation of Poly(EOEOVE) and Poly(EOEOVE-*b*-ODVE)

feed		composition				
EOEOVE (mol/L)	ODVE (mol/L)	EOEOVE (%)	ODVE (%)	M_w	M_n	M_w/M_n
0.13	0	33	0	6000	5300	1.14
0.24	0	52	0	9500	8300	1.15
0.48	0	99	0	18300	15800	1.16
0.13	0.04	31	5	7800	6900	1.13
0.24	0.04	52	4	10800	9300	1.16
0.48	0.04	99	4	19000	16700	1.14

An endotherm is associated with the LCST of thermosensitive polymers, such as poly(NIPAM) and poly(vinyl methyl ether) (*28*, *29*), mainly because of the destruction of water around the hydrophobic groups upon a coil-to-globule transition of the polymer chain at the LCST (*30*). Therefore, we conducted microcalorimetric analyses to estimate the LCST of poly(EOEOVE) and to determine the influence of polymer chain length (Figure 2). Despite differences in molecular weight, these polymers showed similar endotherms of 14−15 J/g for the conformational transition, indicating that the destruction of water associated with the polymers occurred with a similar efficiency. However, the molecular weight affected the transition temperature of the polymers. The polymers with molecular weights of 5300, 8300, and 15 800 exhibited endotherms centered at 45, 41, and 40 °C, respectively. Apparently, the polymer with a higher molecular weight underwent a transition at a lower temperature. It is likely that a longer polymer chain enhances dehydration through efficient intramolecular interactions in addition to intermolecular interactions, resulting in a transition in a lower temperature region.

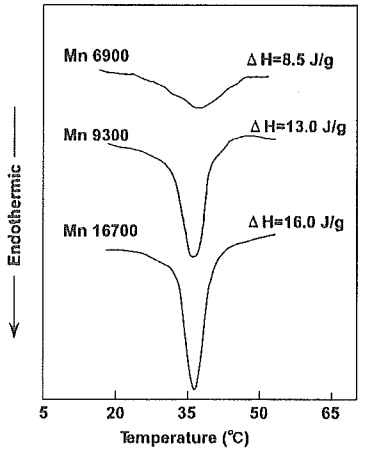

Figure 3. Microcalorimetric endotherms for copoly(EOEOVE–ODVE) with M_n of 6900, 9300 and 16 700 in the presence of EYPC in water. Copolymer/lipid (w/w) ratio was 1/1.

A microcalorimetric analysis was also performed for mixtures of EYPC and copoly(EOEOVE-*b*-ODVE) suspended in water to obtain information about the transition of poly(EOEOVE) chains fixed onto the lipid membrane (Figure 3). As shown in Figure 3, these copolymers on the surface of the lipid membrane showed endotherms in approximately the same temperature region of 36–39 °C, irrespective of the difference in poly(EOEOVE) chain length. In comparison with the transition in aqueous solution, it is apparent that the poly(EOEOVE) chain undergoes a phase transition at a lower temperature. The hydrophobic environment of the lipid membrane periphery may enhance dehydration of the polymer chain, enabling the polymer chain to undergo a transition at a low temperature. In addition, a comparison of endotherms for transitions of these copolymers with the EYPC membrane revealed that the copolymer with a higher molecular weight underwent the transition in a narrow temperature region with a large transition enthalpy, indicating that the longer polymer chain undergoes more efficient transition on the lipid membrane.

3.2. Characterization of Copolymer-Modified Liposomes. We used a mixture of DOPE and EYPC (7:3, mol/mol) as the liposomal lipids because inclusion of DOPE into EYPC liposomes modified with NIPAM copolymers improved their temperature sensitivity (*31*). The liposomes were prepared from mixtures of the lipids and block copolymers. The copolymer/DOPE/EYPC liposomes were extruded through a polycarbonate membrane with a pore size of 100 nm and purified by GPC using a Sepharose 4B column. The amounts of copolymers fixed onto the liposomes are listed in Table 2. Irrespective of poly(EOEOVE) chain length, generally more than 90% of the copolymer added for preparation of the liposome was retained in the liposome after purification by GPC, indicating that four or five octadecyl groups connected to the terminal moiety of the copolymer chain could fix the poly(EOEOVE) chains, although a slightly lower fixation efficiency was observed for liposomes prepared using the copolymer with an M_n of 16 700 and copolymer/lipid ratio of 1.5. The mean diameters of the copolymer-modified liposomes also are listed in Table 2, which possess slightly larger diameters than the pore size of the filter membrane used for the preparation of the liposomes. Since the liposomes containing the copolymer with higher M_n tend to have larger diameters, the chain length of the copolymer may increase the apparent size of the liposomes by assuming an extended conformation on the liposome surface.

Table 2. Characterization of Copoly(EOEOVE–ODVE)-Modified Liposomes[a]

M_n of copolymer	copolymer added (mg/mg lipid)	copolymer fixed (mg/mg lipid)	mean diameter (nm)
6900	0.5	0.44	132
	1.0	0.93	126
	1.5	1.36	132
9300	0.5	0.49	142
	1.0	0.96	139
	1.5	1.47	131
16700	0.5	0.40	157
	1.0	0.89	157
	1.5	1.25	151

[a] Measurements were performed at 20 °C.

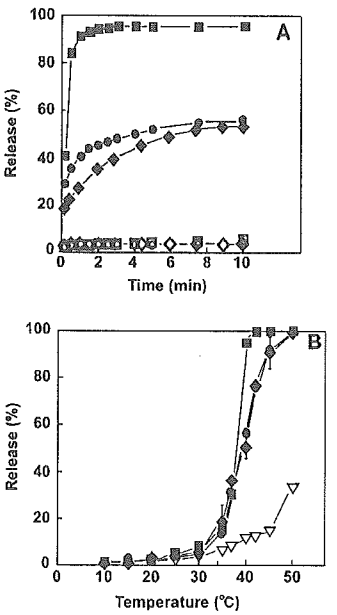

Figure 4. Release of calcein from the copolymer-modified DOPE/EYPC (7/3, mol/mol) liposomes: (A) profiles of calcein release from DOPE/EYPC (7/3, mol/mol) liposomes modified with copoly(EOEOVE-*b*-ODVE) with M_n of 6900 (diamonds), 9300 (circles), and 16 700 (squares) in 10 mM Tris-HCl, 140 mM NaCl, and 1 mM EDTA at 40 °C (solid symbols) and 25 °C (open symbols); (B) percent release of calcein from DOPE/EYPC (7/3, mol/mol) liposomes modified with copoly(EOEOVE-*b*-ODVE) with M_n of 6900 (diamonds), 9300 (circles), and 16 700 (squares) or unmodified DOPE/EYPC (7/3, mol/mol) liposome (triangles) after 10 min of incubation as a function of the incubation temperature. The liposomes were prepared from a copolymer/lipid (0.5/1, w/w) mixture.

3.3. Calcein Release from Copolymer-Modified Liposomes. To estimate first the ability of these block copolymers to sensitize the liposome to temperature and then to understand the effect of chain length of the copolymer on their ability for temperature sensitization of the liposome, we examined the content release behavior of liposomes modified with copoly(EOEOVE-*b*-ODVE) of varying molecular weights. Calcein (formula weight, 622.5) was used as a permeant because this water-soluble dye exhibits considerable self-quenching when entrapped in a liposome at high concentration but fluoresces when released into the outer phase (*31*). Figure 4A shows calcein release profiles from EYPC/DOPE liposomes modified with copolymers at 25 and 40 °C. As shown in Figure 4A, the liposomes did not release calcein at 25

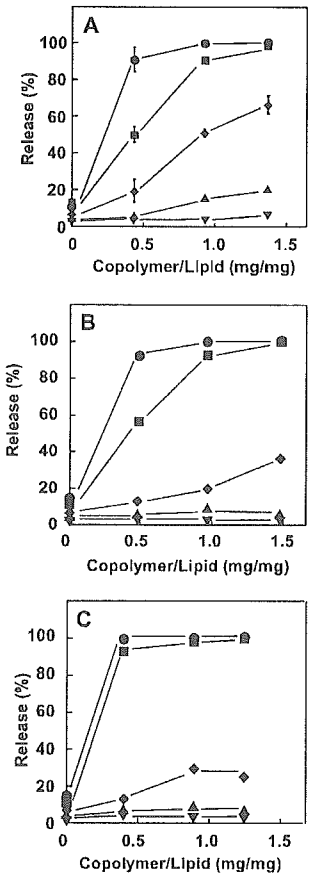

Figure 5. Percent release of calcein from DOPE/EYPC (7/3, mol/mol) liposomes after 10 min of incubation at 25 (▼), 30 (▲), 35 (◆), 40 (■), and 45 (●) as a function of content of copoly(EOEOVE-*b*-ODVE)s with M_n of 6900 (A), 9300 (B), and 16 700 (C).

°C; however, strong release was induced at 40 °C. As shown earlier, the poly(EOEOVE) segment of the copolymer changes its nature from hydrophilic to hydrophobic near 36 °C (Figure 3). Thus, these results imply that a hydrated chain of poly(EOEOVE) does not destabilize the liposomal membrane, but a dehydrated chain interacts with the membrane, enhancing permeation of calcein through the membrane. In addition, liposomes modified with copolymers of higher M_n exhibited more significant content release at 40 °C, indicating that the ability of the poly(EOEOVE) chain to sensitize liposomes increases with chain length. It is noteworthy that the copolymer with a M_n of 16 700 conferred a high degree of temperature sensitivity to liposomes, which achieved complete content release within 1 min.

As shown in Figure 4A, significant release was induced within the first 1 or 2 min. However, the release gradually slowed and approached a constant value after 10 min. The extent of content release after 10 min at varying temperatures was plotted as a function of incubation temperature (Figure 4B). The content release was clearly enhanced above 36 °C, where dehydration of poly(EOEOVE) presumably occurred on the lipid membrane, indicating that the change of the polymer chain from hydrophilic to hydrophobic triggered content release.

Figure 5 depicts the effect of copolymer content of the liposome membrane on calcein release behavior of the liposomes. No remarkable difference in calcein release was observed in liposomes modified with copolymers of different M_n below 30 °C or at 45 °C. These results suggest that highly hydrated or well-dehydrated polymer chains interact with membranes in a similar manner, irrespective of the difference in chain length. In contrast, a significant difference was observed in calcein release at 35 and 40 °C among these copolymer-modified liposomes. The copolymer with an M_n of 6900 possessed significant ability to enhance release at 35 °C, whereas the copolymer with an M_n of 16 700 exhibited a much lower ability to enhance release at the same temperature. In contrast, at 40 °C the copolymer with a high M_n achieved complete release even at a copolymer/lipid ratio of 0.5, whereas the copolymer with a low M_n induced only 50% release at the same copolymer/lipid ratio. As seen in Figure 3, dehydration of the poly(EOEOVE) segment was not complete at these temperatures. For the short chain of poly(EOEOVE), dehydrated segments of the polymer chain may interact with and destabilize the liposome membrane, although the degree of dehydration might be limited at 35 °C. However, for the longer polymer chain, because of its higher conformational freedom, dehydrated segments could associate with each other, resulting in weak interaction with the membrane. In contrast, at 40 °C, the longer polymer chain enables its dehydration more efficiently because of its larger freedom of conformation, resulting in a stronger interaction with the liposome and more significant release of calcein.

3.4. Interaction of Copolymers with Liposome Membrane. The influence of the copolymer on membrane fluidity of the liposome was investigated to obtain information about interactions with the lipid membrane using the fluorescent probes ANS and DPH. These fluorescent molecules are used widely to estimate membrane fluidity and provide information about the surface (ANS) and hydrophobic region (DPH) of the membrane (*32*). The inverse polarization of fluorescence probes (1/*P*) indicated the membrane fluidity (*32*).

For simplicity, EYPC was used as the liposomal lipid for estimation of membrane fluidity. Figure 6A depicts the temperature dependence of membrane fluidity of the liposomes as monitored by ANS. For unmodified liposomes, membrane fluidity increased with temperature. Similarly, the membrane fluidity of liposomes modified with the copolymer with an M_n of 6900 increased with temperature; no change in the temperature dependence of membrane fluidity was observed near the transition temperature. For liposomes modified with copolymers with M_n of 9300 and 16 700, the membrane fluidity increased monotonically up to 40 °C; this increase in membrane fluidity was slightly suppressed near 40 °C. Since this temperature is close to that at which significant enhancement of content release occurred, it is likely that the dehydrated chains of poly(EOEOVE) interact with the lipid membrane and suppress mobility of the lipid molecules. Because suppression was observed only with copolymers of higher molecular weights, the interaction of the copolymer with the membrane may increase with chain length of the poly(EOEOVE) segment. However, a previous study showed more significant suppression of the EYPC membrane upon modification with NIPAM copolymers (*24*, *27*); thus, the interaction of poly(EOEOVE) with the membrane may be relatively weak.

A similar tendency was seen for membrane fluidity as monitored by DPH (Figure 6B). Membrane fluidity of the unmodified EYPC liposome increased monotonically with temperature, whereas increase in membrane fluidity was

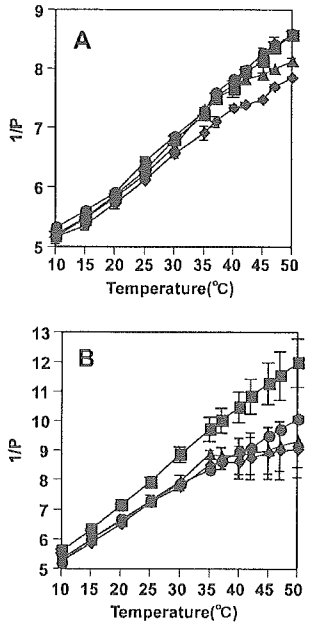

Figure 6. Temperature dependence of membrane fluidity (1/*P*) of EYPC liposomes modified with copoly(EOEOVE-*b*-ODVE)s with M_n of 6900 (●), 9300 (▲), and 16 700 (◆), and unmodified EYPC liposome (■) in 10 mM Tris-HCl and 140 mM NaCl solution (pH7.4) as monitored by ANS (A) and DPH (B). The concentrations of EYPC, ANS, and DPH were 0.4 mM, 4.4 μM, and 0.44 μM, respectively. Copolymer/lipid (w/w) ratio of the liposomes was 0.5/1.

suppressed above 37 °C for membranes having poly(EOEOVE) chains. More significant suppression was observed for membranes modified with copolymers of higher M_n. As mentioned earlier, copolymer chains with higher M_n underwent conformational transition more efficiently than did copolymers with a low M_n. Therefore, the longer chains of poly(EOEOVE) could form a more hydrophobic domain upon the transition and interact more strongly with the membrane. A comparison between membrane fluidities monitored by ANS and DPH showed that the latter indicated more pronounced suppression by the copolymers, implying that the copolymers interact with the hydrophobic region of the membrane more strongly than with the peripheral region of the membrane.

3.5. Retention of Dextran in Copolymer-Modified Liposomes. We examined the effect of temperature on retention of dextran in copolymer-modified liposomes to obtain information about the mechanism of content release induced by the copolymers. The copolymer-modified EYPC or DOPE/EYPC (7/3, mol/mol) liposome containing FITC–dextran with an average molecular weight of 4400 was incubated for 30 min at varied temperatures. Figure 7 shows the percent FITC–dextran remaining in the liposomes after a 30 min incubation as a function of incubation temperature. For copolymer-modified EYPC liposomes, more than 75% of the content was retained in the liposomes even at 50 °C, where the poly(EOEOVE) chain becomes fully dehydrated, indicating that the polymer chain causes only limited defects in the EYPC membrane. In contrast, for copolymer-modified liposomes containing DOPE, only a small portion of the contents remained after incubation above the transition temperature of poly(EOEOVE). Considering that a large molecule with an average molecular weight

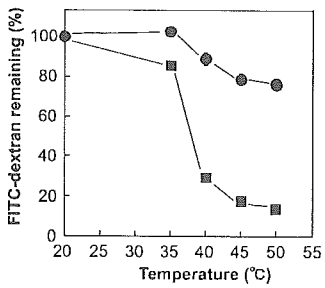

Figure 7. Retention of FITC–dextran from copoly(EOEOVE-*b*-ODVE) (M_n of 16 700) modified EYPC (●) and DOPE/EYPC (7/3, mol/mol) (■) liposomes after 30 min of incubation as a function of incubation temperature. Copolymer/lipid (w/w) ratio was 0.5/1.

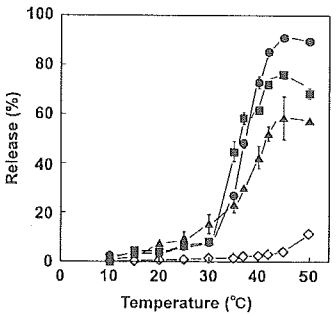

Figure 8. Percent release of calcein from EYPC liposomes modified with copoly(EOEOVE-*b*-ODVE) with M_n of 6900 (triangles), 9300 (squares), and 16 700 (circles) or unmodified EYPC liposome (diamonds) after 10 min of incubation in 10 mM Tris-HCl, 140 mM NaCl, and 1 mM EDTA as a function of the incubation temperature. The liposomes were prepared from a copolymer/lipid (1.5/1, w/w) mixture.

of 4400 was released effectively to the outer phase, it is likely that disintegration of the liposome was induced by the dehydrated polymer chain in the DOPE-containing liposome. It is well-known that EYPC forms a stable bilayer membrane under physiological condition, whereas DOPE has a tendency to form a hexagonal II structure (*33*, *34*). Therefore, it is likely that the interaction with the dehydrated chain of poly(EOEOVE) did not induce a significant defect in the stable bilayer membrane of EYPC but enhanced the transition of the DOPE-containing membrane from a lamellar to a nonlamellar phase, resulting in rupture of the liposome.

3.6. Sensitization of EYPC Liposomes by Copolymer-Modified Liposomes. It has been shown that the interaction between poly(NIPAM) and phosphatidylcholine membranes is not strong enough to induce significant release from the liposomes (*5*, *6*, *35*). Inclusion of DOPE has been shown to improve temperature-sensitive release properties of poly(NIPAM)-modified liposomes (*27*). At the same time, however, the stability of the liposomes decreases because DOPE has a high tendency to form a nonbilayer structure. Therefore, it is highly desired to provide highly temperature-sensitive properties to stable phosphatidylcholine liposomes. Thus, we examined the ability of these copolymers to sensitize EYPC liposomes. As is seen in Figure 8, EYPC liposomes modified with poly(EOEOVE-*b*-ODVE) enhanced release of calcein above 35 °C, indicating that these polymers have an ability to sensitize liposomes with a stable phosphatidylcholine membrane to temperature. In addition, the extent of enhancement of the contents release became more significant for the liposomes modified with the copolymer

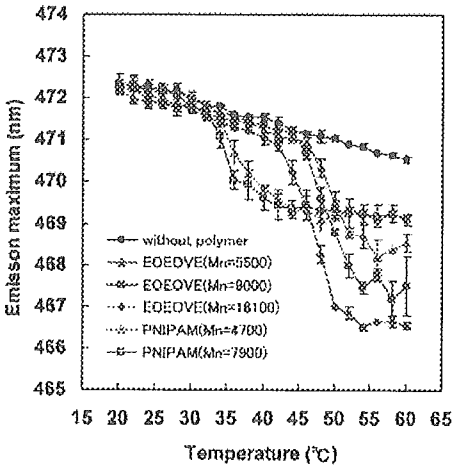

Figure 9. Emission maxima for PyCHO in the absence or presence of poly(NIPAM) or poly(EOEOVE) with varying molecular weights in water. The concentrations of PyCHO and the copolymers were 1 μM and 0.2 mg/mL, respectively. Poly(NIPAM)s with M_n of 4700 and M_w of 10 000 and with M_n of 7900 and M_w 23 000 were used. Poly(EOEOVE)s with M_n of 5500 and M_w of 6300, M_n of 9000 and M_w of 10 400, and M_n of 16100 and M_w of 18 400 were used.

of a higher molecular weight. In particular, the liposomes having a copolymer with a molecular weight of 16 700 exhibited a sharp and intensive contents release around the polymer transition temperature. This result clearly indicates that the poly(EOEOVE-*b*-ODVE) is very useful for obtaining stable phosphatidylcholine liposomes with temperature-sensitive properties.

The poly(EOEOVE-*b*-ODVE) was shown to be able to sensitize EYPC liposomes. This implies that poly(EOEOVE) forms a more hydrophobic domain than poly(NIPAM) does after their conformational transition because the contents release from the liposomes would be induced mainly by hydrophobic interaction between the liposome membrane and the dehydrated polymer chains. To confirm it, we further examined the hydrophobicity of domains formed by these polymers above the transition temperature using PyCHO. This molecule is known to change the wavelength of the emission maximum (λ_{max}) of the fluorescence, depending on polarity of the solvent (*26*). By using this property of PyCHO, Schild and Tirrell detected collapse of the backbone of the homopolymer and copolymers of NIPAM (*26*).

Two poly(NIPAM)s with M_n of 4700 and M_w of 10 000 and with M_n of 7900 and M_w of 23 000 were compared with three poly(EOEOVE)s with M_n of 5500 and M_w of 6300, M_n of 9000 and M_w of 10 400, and M_n of 16 100 and M_w of 18 400. As is seen in Figure 9, λ_{max} of PyCHO dissolved in an aqueous solution slightly decreased with increasing temperature in the absence of the polymer. In contrast, in the presence of the polymers, a marked blue shift above the LCST was observed around 35 °C for poly(NIPAM)s and at 44–46 °C for poly(EOEOVE)s, indicating that these polymers formed hydrophobic domains at these temperatures. As judged from the extent of emission blue shift, hydrophobicity of domains formed by poly(NIPAM)s is hardly affected by their molecular weights. In contrast, hydrophobicity of domains formed by poly(EOEOVE) increased with increasing molecular weight. This is consistent with the fact that the liposomes having longer chains of poly(EOEOVE) exhibited more intensive contents release (Figures 4 and 8) because polymer chains with greater hydrophobicity could destabilize liposome membrane more strongly and cause more intensive permeation of the contents through the membrane. In addition, when the extent of blue shift is compared between poly(NIPAM) and poly(EOEOVE), apparently the latter showed a more significant blue shift. For example, the poly(EOEOVE) with M_n of 5500 exhibited a larger blue shift than poly(NIPAM) with M_n of 7900. This result indicates that poly(EOEOVE) is more potent for sensitization of liposomes to temperature than poly(NIPAM), which has been used for the same purpose.

4. CONCLUSIONS

We synthesized three types of copoly(EOEOVE-*b*-ODVE) with varying chain lengths of poly(EOEOVE) segments, which become hydrophilic or hydrophobic depending on the local temperature, via living cationic polymerization. We also investigated the influence of chain length of the poly(EOEOVE) segments on their ability to sensitize liposomes. Irrespective of poly(EOEOVE) chain length, the copolymers on the surface of the liposomes enhanced the release of calcein entrapped in the EYPC/DOPE liposomes above 35°C, which corresponds to the transition temperature of the poly(EOEOVE) segment of the copolymer on the lipid membrane. However, a longer chain possessed a greater ability to enhance content release within a narrow temperature region near the transition temperature. Thus, the copolymer with an M_n of 16 700, which is the highest molecular weight among the copolymers prepared in this study, produced sharp and rapid control of content release at the transition temperature of the poly(EOEOVE) segment. NIPAM copolymers have been used for the sensitization of liposomes (*6*–*9*). However, we have shown that poly(EOEOVE-*b*-ODVE) can also be used to sensitize liposomes to temperature. Because the copolymers used in this study were prepared by living cationic polymerization, they have the advantage of allowing control of the molecular architecture. In addition, the thermosensitive moiety of poly(EOEOVE-*b*-ODVE) shares a common structural unit with poly(ethylene glycol), which is a widely used, biocompatible polymer. In addition, it is suggested that the block copolymers have greater ability to sensitize stable liposomes than poly(NIPAM). The localized hyperthermia can be achieved by the use of microwave or radiofrequency energy or phased array ultrasound; energy focused on the tumor results in an increase in local temperature (*36*). Therefore, when coupled with local hyperthermia, these liposomes are expected to deliver anticancer drugs specifically to the target tumor. We are currently studying heat-induced control of delivery of anticancer drugs, such as doxorubicin, using the copolymer-modified liposomes and evaluating their usefulness as a site-specific delivery system of anticancer drugs.

LITERATURE CITED

(1) Lian, T., and Ho, R. J. Y. (2001) Trends and developments in liposome drug delivery systems. *J. Pharm. Sci. 90*, 667–680.

(2) Yatvin, M. B., Weinstein, J. N., Dennis, W. H., and Blumenthal, R. (1978) Design of liposomes for enhanced local release of drugs by hyperthermia. *Science 202*, 1290–1293.

(3) Huang S. K., Stauffer, P. R., Hong, K., Guo, J. W. H., Phillips, T. L., Huang, A., and Papahadjopoulos, D. (1994) Liposomes and hyperthermia in mice: increased tumor uptake and therapeutic efficacy of doxorubicin in sterically stabilized liposomes. *Cancer Res. 54*, 2186–2191.

(4) Needham, D., and Dewhirst, M. W. (2001) The development of a new temperature-sensitive drug delivery system for the treatment of solid tumors. *Adv. Drug Delivery Rev. 53*, 285–305.

(5) Kono, K., Hayashi, H., and Takagishi, T. (1994) Temperature-sensitive liposomes: liposomes bearing poly(*N*-isopropylacrylamide). *J. Controlled Release 30*, 69−75.
(6) Kono, K. (2001) Thermosensitive polymer-modified liposomes. *Adv. Drug Delivery Rev. 53*, 307−319.
(7) Kitano, H., Maeda, Y., Takeuchi, S., Ieda, K., and Aizu, Y. (1994) Liposomes containing amphiphilic poly-(*N*-isopropylacrylamides) prepared by using a lipophilic radical initiator. *Langmuir 10*, 403−406.
(8) Wu, X. S., Hoffman, A. S., and Yager, P. (1991) Conjugation of phosphatidylethanolamine to poly(*N*-isopropylacrylamide) for potential use in liposomal drug delivery systems. *Polymer 33*, 4659−4662.
(9) Polozova, A., and Winnik, F. M. (1997) Mechanism of the interaction of hydrophobically-modified poly-(*N*-isopropylacrylamides) and liposomes. *Biochim. Biophys. Acta 1326*, 213−224.
(10) Chandaroy, P., Sen, A., and Hui, S. W. (2001) Temperature-controlled content release from liposomes encapsulating Pluronic F127. *J. Controlled Release 76*, 27−37.
(11) Ringsdorf, H., Sackmann, E., Simon, J., and Winnik, F. M. (1993) Interactions of liposomes hydrophobically-modified poly(*N*-isopropylacrylamides): an attempt to model the cytoskeleton. *Biochim. Biophys. Acta 1153*, 335−344.
(12) Hayashi, H., Kono, K., and Takagishi, T. (1999) Temperature sensitization of liposomes using copolymers of *N*-isopropylacrylamide. *Bioconjugate Chem. 10*, 412−418.
(13) Hayashi, H., Kono, K., and Takagishi, T. (1998) Temperature-dependent associating property of liposomes modified with a thermosensitive polymer. *Bioconjugate Chem. 9*, 382−389
(14) Hayashi, H., Kono, K., and Takagishi, T. (1996) Temperature-controlled release property of phospholipid vesicles bearing a thermo-sensitive polymer. *Biochim. Biophys. Acta 1280*, 127−134.
(15) Masci, G., Giacomelli, L., and Crescenzi, V. (2004) Atom transfer radical polymerization of *N*-isopropylacrylamide. *Macromol. Rapid Commun. 25*, 559−564.
(16) Ray, B., Isobe, Y., Morioka, K., Habaue, S., Okamoto, Y., Kamigaito, M., and Sawamoto, M. (2003) Synthesis of isotactic poly(*N*-isopripylacrylamide) by RAFT polymerization in the presence of Lewis acid. *Macromolecules 36*, 543−545.
(17) Convertine, A. J., Ayres, N., Scales, C. W., Lowe, A. B., and McCormick, C. L. (2004) Facile, controlled, room-temperature RAFT polymerization of N-isopropylacrylamide. *Biomacromolecules 5*, 1177−1180.
(18) Yusa, S., Shimada, Y., Mitsukami, Y., Yamamoto, T., and Morishima, Y. (2004) Heat-induced association and dissociation behavior of amphiphilic diblock copolymers synthesized via reversible addition−fragmentation chain transfer radical polymerization. *Macromolecules 37*, 7507−7513.
(19) Aoshima, S., Oda, H., and Kobayashi, E. (1992) Synthesis of thermally-induced phase separating polymer with well-defined polymer structure by living cationic polymerization. I. Synthesis of poly(vinyl ether)s with oxyethylene units in the pendant and its phase separation behavior in aqueous solution. *J. Polym. Sci., Part A: Polym. Chem. 30*, 2407−2413.
(20) Aoshima, S., and Sugihara, S. (2000) Syntheses of stimuli-responsive block copolymers of vinyl ethers with side oxyethylene groups by living cationic polymerization and their thermosensitive physical gelation. *J. Polym. Sci.: Part A: Polym. Chem. 38*, 3962−3965.
(21) Aoshima, S., and Hashimoto, K. (2001) Stimuli-responsive block copolymers with polyalcohol segments: syntheses via living cationic polymerization of vinyl ethers with a silyloxyl group and their thermoreversible physical gelation. *J. Polym. Sci.: Part A: Polym. Chem. 39*, 746−750.
(22) Aoshima, S.; Higashimura, T. (1986) Living cationic polymerization of vinyl monomers by organoaluminum halides. 1. Etalsl2/ester initiating systems for living polymerization of vinyl ethers. *Polym. Bull. 15*, 417−423.
(23) Kono, K., Nakai, R., Morimoto, K., and Takagishi, T. (1999) Thermosensitive polymer-modified liposomes that release contents around physiological temperature. *Biochim. Biophys. Acta 1416*, 239−250.
(24) Yoshino, K., Kadowaki, A., Takagishi, T., and Kono, K. (2004) Temperature-sensitization of liposomes by use of *N*-isopropylacrylamide copolymers with varying transition endotherms. *Bioconjugate Chem. 15*, 1102−1109.
(25) Bartlett, G. R. (1959) Phosphrus assay in column chromatography. *J. Biol. Chem. 234*, 466−468.
(26) Schild, H., and Tirrell, D. A. (1991) Microbeterogeneous solutions of amphiphilic copolymers of *N*-isopropylacrylamide. *Langmuir 7*, 1319−1324.
(27) Kono, K., Henmi, A., Yamashita, H., Hayashi, H., and Takagishi, T. (1999) Improvement of temperature-sensitivity of poly(*N*-isopropylacrylamide)-modified liposomes, *J. Controlled Release 59*, 63−75.
(28) Heskins, M., and Guillet, J. E. (1968) Solution properties of poly(*N*-isopropylacrylamide). *J. Macromol. Sci., Chem., A2*, 1441−1455.
(29) Schild, H. G., and Tirrell, D. A. (1990) Microcalorimetric detection of lower critical solution temperatures in aqueous polymer solutions. *J. Phys. Chem. 94*, 4352−4356.
(30) Feil, H., Bae, Y. H., Feijen, J., and Kim, S. W. Effect of comonomer hydrophilicity and ionization on the lower critical solution temperature of *N*-isopropylacrylamide copolymers. *Macromolecules 26*, 2496−2500.
(31) Allen, T. M. (1983) Calcein as a tool in liposome methodology. In *Liposome Technology, Vol. III. Targeted Drug Delivery and Biological Interaction* (Gregoriadis, G., Ed.) pp 177−182, CRC Press: Boca Raton, FL.
(32) Ohtoyo, T., Shimagaki, M., Otoda, K., Kimura, S., and Imanishi, Y. (1988) Change in membrane fluidity induced by lectin-mediated phase separation of the membrane and agglutination of phospholipids vesicles containing glycopeptides. *Biochemistry 27*, 6458−6463.
(33) Cullis, P. R., and De Kruiff, B. (1979) Lipid polymorphism and the functional roles of lipids in biological membranes. *Biochim. Biophys. Acta 559*, 399−420.
(34) Litzinger, D. C., and Huang, L. (1992) Phosphatidylethanolamine liposomes: drug delivery, gene transfer and immunodiagnostic applications. *Biochim. Biophys. Acta 1113*, 201−227.
(35) Kim, J.-C., Bae, S. K., and Kim, J.-D. (1997) Temperature-sensitivity of liposomal lipid bilayers mixed with poly(*N*-isopropylacrylamide-*co*-acrylic acid). *J. Biochem. (Tokyo) 121*, 15−19.
(36) Mills J. K., and Needham, D. (2004) The materials engineering of temperature-sensitive liposomes. *Methods Enzymol. 387*, 82−113.

BC050004Z

Preparation of Efficient Gene Carriers Using a Polyamidoamine Dendron-Bearing Lipid: Improvement of Serum Resistance

Toshinari Takahashi,† Atsushi Harada,† Nobuhiko Emi,‡ and Kenji Kono*,†

Department of Applied Chemistry, Graduate School of Engineering, Osaka Prefecture University, 1-1 Gakuen-cho, Sakai, Osaka 599-8531, Japan, and Department of Hematology, Nagoya University Graduate School of Medicine, Nagoya, Aichi 466–8550, Aichi, Japan. Received January 20, 2005; Revised Manuscript Received July 4, 2005

In a previous study, we developed a novel cationic lipid consisting of polyamidoamine dendron of third generation and two dodecyl chains, designated as DL-G3, which in combination with a fusogenic lipid dioleoylphosphatidylethanolamine (DOPE) achieves efficient transfection of CV1 cells by synergetic action of the proton sponge effect and membrane fusion. This study examines the effect of serum on the transfection activity of the DL-G3–DOPE–plasmid DNA lipoplexes. The transfection activity of a lipoplex with a composition optimized in the absence of serum decreased markedly in the presence of serum. However, the lipoplexes that induce efficient transfection in the presence of serum were obtainable by controlling the charge ratio of the primary amine of the DL-G3 to the phosphate group (N/P ratio) and DOPE content. The complex, which exhibited the highest transfection activity in the presence of serum, has a lower N/P ratio and higher DOPE content than that optimized in the absence of serum. Whereas disintegration of these complexes was induced by addition of heparin, which is a polysaccharide with negatively charged groups, the complex that retained transfection activity in the presence of serum required more negative charges of heparin for complex disintegration. That result implies its higher stability against negatively charged serum proteins. Comparison of the serum-resistant complex with some commercially available transfection reagents, such as Lipofectamine and SuperFect, indicates that the DL-G3 complex achieved more efficient transfection of these cells in the presence of serum.

INTRODUCTION

Development of nonviral systems that introduce therapeutic genes efficiently into a target cell has been highly desired for the establishment of gene therapy. Synthetic systems based on lipids or polymers with positive charges have been studied actively for this purpose, but their activity still requires improvement. These systems can form complexes with plasmid DNA, which are termed lipoplexes (lipid-based complexes) and polyplexes (polymer-based complexes) through electrostatic interactions (*1*, *2*). These complexes can interact strongly with cells through electrostatic interactions. They are taken up by the cells through the endocytic pathway. Avoidance of plasmid DNA degradation in the lysosome and its transfer into cytosol are considered to be a key process for efficient transfection. Cationic lipid-based systems are considered to promote this process by fusing with and destabilizing the endosomal membrane with the help of fusogenic lipids such as dioleoylphosphatidylethanolamine (DOPE). Some synthetic cationic polymers such as poly(ethylenimine) (*3*, *4*) and polyamidoamine dendrimers (*5*) also induce efficient transfection of cells by enhancing the transfer of plasmid DNA into cytosol through the so-called proton sponge effect (*6*).

In a previous study (*7*), we developed a novel type of cationic lipids that consist of two dodecyl groups and a polyamidoamine dendron as a headgroup because these dendron-bearing lipids can form lipoplexes with DOPE and plasmid DNA, which achieve efficient transfection of cells by the synergetic action of membrane fusion and the proton sponge effect. In fact, in combination with DOPE, the lipid with the third generation dendron, DL-G3 (Figure 1), achieved more efficient transfection of CV1 cells, a green monkey kidney cell line, than widely used nonviral vectors.

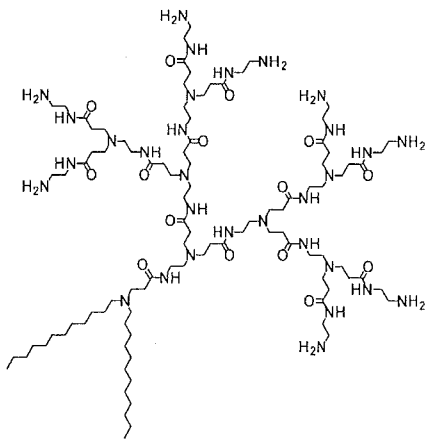

Figure 1. Structure of DL-G3.

A major problem for the cationic lipid/polymer-based gene carriers is their sensitivity to serum proteins: their transfection activity is lowered dramatically in the presence of serum proteins (*8*–*14*). Their complexes with plasmid DNA interact with serum components and cause

* Corresponding author. E-mail: kono@chem.osakafu-u.ac.jp. Tel: +81-722549330. Fax: +81-722549913.
† Osaka Prefecture University.
‡ Nagoya University Graduate School of Medicine.

10.1021/bc050012f CCC: $30.25
Published on Web 08/27/2005

their disintegration, resulting in plasmid DNA release and its degradation (*12*−*15*). Therefore, optimal transfection with these systems must be performed in the absence of serum. Such a serum-sensitive property of the cationic lipid/polymer-based gene carriers apparently restricts their in vivo application and reduces their usefulness as a vector for gene therapy.

To overcome the inhibitory effect of serum on transfection mediated by these gene carriers, many efforts have been made by various approaches. Among them are enhancement of cellular uptake of the complexes through endocytosis by increasing positive charges of the complexes (*12*, *16*) or by attaching target cell specific ligands to the complexes (*17*, *18*), and promotion of transfer of endocytosed genes into cytosol by conjugation of membrane disruptive molecules with the complexes (*17*, *19*, *20*, *21*).

In a previous study, we examined transfection activity of the lipoplexes containing dendron-bearing lipids in the absence of serum. However, considering the strong ability of these dendron-bearing lipid-based lipoplexes to enhance transfer of the gene into cytosol and controllability of their charge density by changing their composition, it is expected that these lipoplexes could achieve efficient transfection in the presence of serum proteins. Therefore, this study is particularly intended to produce lipoplexes that can achieve efficient transfection using DL-G3 and DOPE. Their lipoplex with an optimized composition was found to possess a much higher activity than some commercially available transfection reagents, such as Lipofectamine and SuperFect. We describe the importance of both the ratio of the primary amines of the DL-G3 to the phosphate groups of plasmid DNA and the content of DOPE of lipoplexes for the production of lipoplexes with serum resistance.

EXPERIMENTAL PROCEDURES

General Methods. DOPE was kindly donated by Nippon Oil and Fats Co. (Tokyo, Japan). Fetal calf serum (FCS) was obtained from JRH Biosciences (Tokyo, Japan). Dulbecco's modified Eagle's medium (DMEM) was from Nissui Pharmaceutical (Tokyo, Japan). Tris(hydroxymethyl)aminomethane (Tris) was obtained from Kishida Chemical (Osaka, Japan). Heparin sodium salt was purchased from Sigma (St. Louis, MO). Agarose was purchased from nacalai tesque (Kyoto, Japan). Ethidium bromide was purchased from Wako Pure Chemical Industries (Osaka, Japan). Lipofectamine and SuperFect were purchased from Invitrogen (Carlsbad, CA) and Qiagen (Hilden, Germany), respectively. DL-G3 was synthesized by the procedure previously described (*7*).

Preparation of Lipoplexes. To a dry thin membrane of a mixture of the DL-G3 and a given amount of DOPE was added phosphate-buffered saline (PBS), and the mixture was sonicated for 2 min using a bath-type sonicator to afford a lipid suspension. Plasmid DNA p10, which contains a firefly luciferase coding sequence derived from pGL3-basic (Promega, Madison, WI) between Rous sarcoma virus LTR and polyadenylation signal, (1 μg), was dissolved in 20 mM Tris-HCl buffer (pH 7.4, 50 μL), was mixed with the lipid suspension (50 μL), and incubated for 30 min at room temperature to afford a lipoplex with a given ratio of primary amino group of DL-G3 to DNA phosphate (N/P ratios).

Transfection. Transfection of CV1 cells was done according to the following procedures unless otherwise noted in the text. The cells were seeded in 0.5 mL of DMEM supplemented with 10% FCS in 24-well culture plates at 5.0×10^4 cells per well the day before transfection. The cells were washed with PBS containing 0.36 mM $CaCl_2$ and 0.42 mM $MgCl_2$ [PBS(+)] and then covered with DMEM supplemented with a given amount of FCS (1 mL). The lipoplex-containing plasmid DNA (1 μg) was added gently to the cells and incubated at 37 °C for 4 h. Then, the cells were rinsed with PBS(+), covered with DMEM containing 10% FCS, and incubated at 37 °C. After 40 h, the cells were lysed by adding 50 μL of Luc-PGC-50 detergent (Toyo Ink, Tokyo, Japan). A 20 μL aliquot from each dish was used for one luciferase assay using a kit (Toyo Ink) and a Lumat LB9507 luminometer (Berthold, Bad Wildbad, Germany). The protein content of the lysate was measured by Coomassie Protein Assay Reagent (Pierce, IL) using bovine serum albumin as the standard. Transfection by Lipofectamine and SuperFect was performed according to their protocols recommended by the manufacturers. Transfection of HepG2 cells was performed according to the above procedure except that the cells were seeded 2 days before the transfection.

Interaction of the Lipoplexes with Heparin. The DL-G3−DOPE lipoplexes with varying N/P ratios and DOPE contents were prepared by mixing plasmid DNA (1 μg) dissolved in 20 mM Tris-HCl buffer (2.5 μl) and lipid suspension (2.5 μL). After 30 min-incubation at room temperature, the DL-G3−DOPE lipoplexes were added to a given amount (0−2 μg) of heparin dissolved in PBS (5 μL) and incubated for 30 min at room temperature. The samples (10 μL) were electrophoresed on 0.6 wt % agarose gel in 40 mM Tris, 20 mM sodium acetate, and 2 mM EDTA buffer (pH 8.0) containing 1 μg/mL ethidium bromide at 100 V for 30 min. The ethidium bromide-stained bands were visualized using a LAS-1000UVmini (FUJIFILM, Japan) and analyzed with Science Lab 2003 Multi Gauge software (FUJIFILM, Japan).

RESULTS AND DISCUSSION

Effects of Lipoplex Composition on Transfection Activity in the Presence of Serum. Our previous study developed cationic lipids that comprise two dodecyl groups and polyamidoamine dendron of varying generations because we expected that these lipids can form lipoplexes, which achieve an efficient transfection of cells through the synergy of membrane fusion and the proton sponge effect, with DOPE (*7*). When mixed with DOPE, one dendron-bearing lipid, DL-G3, induced transfection of CV1 cells more efficiently than a widely used lipoplex consisting of DC-chol and DOPE in a medium without serum.

We have already established the composition of a lipoplex composed of DL-G3, DOPE, and plasmid DNA with high transfection activity. Specifically, we described lipoplexes with an N/P ratio of 5 and DL-G3/DOPE ratio of 1/5 (*7*). Thereby, we first examined the effect of serum concentration on transfection activity of DL-G3−DOPE lipoplexes with that composition. Figure 2 depicts luciferase activity of CV 1 cells treated with the lipoplex in a medium with varying serum contents. As Figure 2 shows, the presence of even 10% of serum abolished the transfection activity of the DL-G3−DOPE lipoplex. Many studies have revealed that the transfection activity of lipoplexes is reduced dramatically in the presence of serum by interaction between lipoplexes and serum proteins (*12*−*15*). This result indicates that the DL-G3−DOPE lipoplex with this composition is as highly serum-sensitive as other types of cationic lipid-based vectors.

As mentioned previously, the optimum composition of the DL-G3−DOPE lipoplex was established under condi-

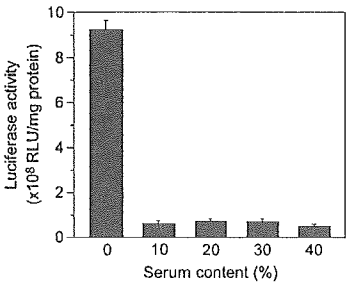

Figure 2. Effect of serum on transfection of CV1 cells mediated by the DL-G3–DOPE lipoplex with N/P ratio of 5 and DOPE/DL-G3 ratio of 5. The cells (5×10^4) were treated with the lipoplexes containing 1 μg of DNA in the medium with varying contents of FCS. Each bar represents the mean ± SD ($n = 3$).

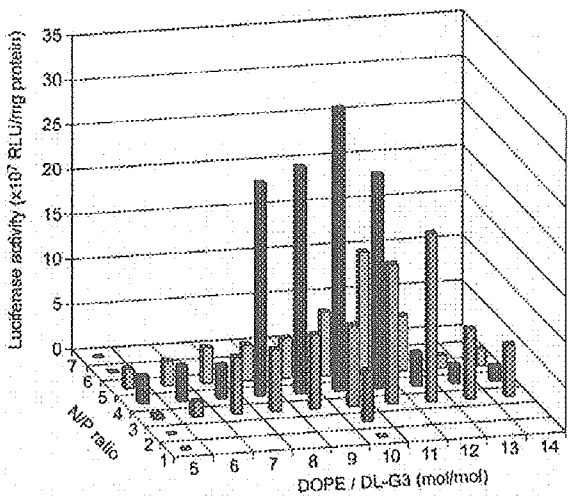

Figure 3. Influences of N/P and DOPE/DL-G3 ratios of lipoplexes on their transfection activity. The cells (5×10^4) were treated with the lipoplexes containing 1μg DNA in the presence of 9.1% FCS. Each bar represents the mean ($n = 4$).

tions without serum. Therefore, the optimum composition of the lipoplex for transfection in the presence of serum might differ from the composition optimized in the absence of serum. For that reason, we next attempted the optimization of the composition of the DL-G3–DOPE lipoplex in the presence of serum (Figure 3).

Inclusion of DOPE in the lipoplex is important because this lipid provides fusion ability to the lipoplex (*22*, *23*). We prepared dispersions of mixtures of DL-G3 and DOPE with varying molar ratios and incubated them with plasmid DNA to obtain lipoplexes with varying DOPE contents at varying N/P ratios. Expression of luciferase in the CV 1 cells treated with these lipoplexes is shown in Figure 3. As that figure shows, the cellular expression of luciferase is dependent on the lipoplex's DOPE content. For example, when the lipoplexes with an N/P ratio of 4 were used, the cellular luciferase activity increased 10-fold as the DOPE content of the lipoplex increased from 5 to 10. However, higher DOPE content of the lipoplexes eliminated their activity. Because DOPE is an electronically neutral lipid, the charge density of the lipoplexes decreases with increasing DOPE content, thereby reducing their affinity to the cellular surface. A similar tendency was shown by lipoplexes with N/P ratios of 3 and 5, but their maximum activities were apparent at DOPE/DL-G3 ratios of 12 and 11 for lipoplexes with the N/P ratios of 3 and 5, respectively. These results indicate that inclusion of DOPE is crucial to obtain potent lipoplexes for use in the presence of serum.

On the other hand, the N/P ratio is another important factor which affects lipoplex activity. As Figure 3 shows, transfection activity of the DL-G3–DOPE lipoplexes changed remarkably depending on the N/P ratio. For lipoplexes with the DOPE/DL-G3 ratio of 10, the activity increases concomitant with an increasing N/P ratio and becomes greatest at the ratio of 4. The transfection activity of the DL-G3–DOPE lipoplexes was affected markedly by both the DOPE/DL-G3 and N/P ratios. However, Figure 3 illustrates that a lipoplex with a DOPE/DL-G3 ratio of 10 and the N/P ratio of 4 exhibited the highest activity in the presence of serum.

As mentioned previously, the lipoplex optimized in the absence of serum has an N/P ratio of 5 and a DOPE/DL-G3 ratio of 5. Compared with this, the lipoplex optimized in the presence of serum has a slightly lower N/P ratio and a two-times-higher DOPE/DL-G3 ratio. Both the lower N/P ratio and the higher DOPE content mean that the lipoplex obtained in this study has a lower charge density than the lipoplex optimized in the absence of serum. The electrostatic force is likely to play an important role in interaction of the lipoplex with serum proteins. Therefore, the lower charge density of the lipoplex may contribute to its weaker interaction with serum proteins and prevent the loss of transfection activity induced by interaction with serum proteins. Indeed, the interaction of the lipoplex with the cellular membrane is based on their electrostatic interaction. For that reason, the low charge density of the lipoplex may also cause a weak interaction with the cell that could result in a lower transfection activity. However, the higher DOPE content of the lipoplex might increase fusion ability of the lipoplex, which could compensate the reduced affinity. As a result, the lipoplex obtained in this study exhibited the high transfection activity.

Figure 4 illustrates the influence of serum concentration on transfection activity of the DL-G3–DOPE lipoplexes optimized in the presence of serum and absence of serum. When serum was absent, both lipoplexes exhibited similar and high transfection activities (Figure 4A), though the activity of the lipoplex optimized in the presence of serum was somewhat higher than that of the lipoplex optimized in the absence of serum. This may be due to the difference of the procedures for optimization of these lipoplexes (*7*). When the serum was present, both lipoplexes reduced the transfection activity. However, the extent of reduction of that activity differed between these lipoplexes. As Figure 4B shows, the lipoplex optimized in the absence of serum retained only 7% of the original activity when 10–40% of serum was contained in the medium of transfection. In contrast, the lipoplex prepared in this study exhibited 20–30% of the original activity under the same conditions. Consequently, we infer that the DL-G3–DOPE lipoplex with the low N/P ratio and the high DOPE content are more resistant to serum.

Interaction of Lipoplexes with Heparin. As mentioned above, the serum-resistance of DL-G3–DOPE lipoplexes was affected significantly by the N/P ratio and the DOPE content. Transfection activity of the lipoplex with the N/P ratio of 5 and the DOPE/DL-G3 ratio of 5 was diminished strongly by serum, whereas the lipoplex with a slightly lower N/P ratio and a higher DOPE content can retain its activity in the presence of serum.

Inactivation of the DL-G3–DOPE lipoplex in the presence of serum is considered to be induced mainly by electrostatic interaction between the lipoplexes with negatively charged serum proteins. In fact, disintegration

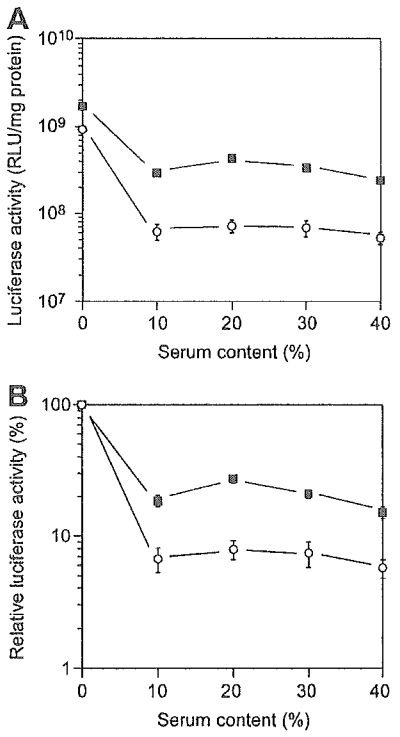

Figure 4. Serum-induced reduction of transfection activity for DL-G3–DOPE lipoplex with N/P ratio of 5 and DOPE/DL-G3 ratio of 5 (○) and DL-G3–DOPE lipoplex with N/P ratio of 4 and DOPE/DL-G3 ratio of 10 (■). Cellular luciferase activity (A) and percentage of cellular luciferase activity in the absence of serum (B) were shown as a function of serum content of the transfection medium. The cells (5×10^4) were treated with DL-G3–DOPE lipoplexes containing 1μg DNA. Each point represents the mean ± SD (n = 3).

of lipoplexes associated with the release of plasmid DNA has often been observed in the presence of serum because the plasmid DNA bound to the cationic lipid molecules is replaced by the negatively charged serum proteins (*12*–*15*).

Some polyanions, such as heparin and dextran sulfate, are also known to dissociate DNA from lipoplexes (*24*, *25*). They have been used to estimate the stability of the lipoplexes. Therefore, we examined the effect of addition of heparin on dissociation of plasmid DNA from the DL-G3–DOPE lipoplexes to evaluate their stability using agarose gel retardation assay (Figure 5). In this experiment, lipoplexes with varying N/P ratios and DOPE/DL-G3 ratios were incubated with varying amounts of heparin for 30 min, then electrophoresed on an agarose gel. As Figs. 5A–C show, a band corresponding to free plasmid DNA appeared as the amount of heparin added to the lipoplexes was increased, indicating that these lipoplexes were disintegrated by interaction with heparin.

Liberation of plasmid DNA was caused mainly by their electrostatic interaction. Therefore, we investigated the correlation between the amount of released plasmid DNA and the charge balance of the mixture of the lipoplex and heparin. Heparin is known to be a highly sulfated glycosaminoglycan consisting of (1 → 4)-*O*-(α-L-idopyranosyluronic acid 2-sulfate)–(1→4)-(2-deoxyl-2-sulfamino-α-D-glucopyranosyl 6-sulfate) as a major repeating unit (*26*, *27*). Thus, we calculated the amount of negative charge of heparin by assuming the structure of heparin as repeats of this disaccharide unit. Figure 5D depicts

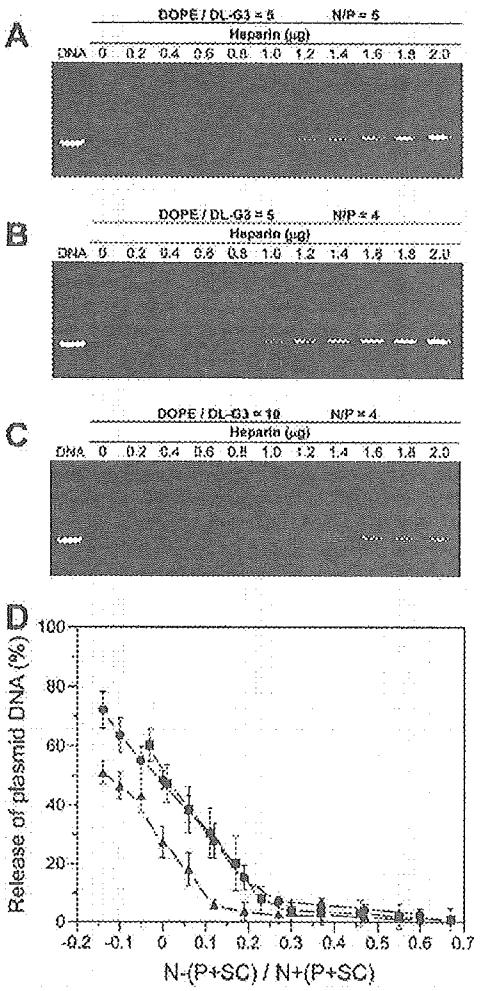

Figure 5. Agarose gel electrophoresis of DL-G3–DOPE lipoplexes with N/P ratio of 5 and DOPE/DL-G3 ratio of 5 (A), with N/P ratio of 4 and DOPE/DL-G3 ratio of 5 (B) and with N/P ratio of 4 and DOPE/DL-G3 ratio of 10 (C) in the presence of varying amounts of heparin. (D) Percent release of plasmid DNA from DL-G3–DOPE lipoplexes with varying compositions as a function of difference between negative and positive charges of lipoplexes normalized by their total charge: ■, lipoplex with N/P ratio of 5 and DOPE/DL-G3 ratio of 5; ●, lipoplex with N/P ratio of 4 and DOPE/DL-G3 ratio of 5; ▲, lipoplex with N/P ratio of 4 and DOPE/DL-G3 ratio of 10. Each point represents the mean ± SD (n = 3). N, P, and SC represent amounts of charge of the primary amine of the DL-G3, phosphate group of DNA, and total of sulfonate and carboxyl groups of heparin, respectively.

the percentage of released plasmid DNA as a function of the difference between positive and negative charges of the lipoplex–heparin mixture normalized by its total amount of charge. Figure 5D shows the curve for a lipoplex with an N/P ratio of 5 and with a DOPE/DL-G3 ratio of 5 (■). It also depicts the curve for a lipoplex with an N/P ratio of 4 and a DOPE/DL-G3 ratio of 5 (●). They are approximately identical. This result indicates that the liberation of plasmid DNA from these lipoplexes is controlled simply by their charge balance when the DOPE content of the lipoplexes was the same. However, comparison between the lipoplex with the N/P ratio of 4 and the DOPE/DL-G3 ratio of 5 and the lipoplex with the same N/P ratio and with the DOPE/DL-G3 ratio of

10 (▲) indicates that the latter requires more negative charge than the former for liberation of plasmid DNA, suggesting that inclusion of DOPE contributes to lipoplex stability. Probably, DOPE molecules inserted in the complex could stabilize the electrostatic binding between DNA and the DL-G3 by hydrophobic interaction and cover the DNA efficiently, isolating it from the outer environment and suppressing interaction with negatively charged molecules. Therefore, it is likely that the high content of DOPE in the lipoplex with the N/P ratio of 4 and the DOPE/DL-G3 ratio of 10 can enhance stability of the lipoplex and provide a high serum-resistant property to the lipoplex.

In addition, particle size of the complexes can be another factor that affects interaction of the lipoplexes with serum protein and their serum-sensitivity. Thus, we measured size of the lipoplexes by DLS. The sizes of serum-resistant and serum-sensitive lipoplexes were shown to be 767 ± 183 nm and 616 ± 193 nm, respectively. The slightly smaller size of the latter may enhance its serum sensitivity to some extent, because it would interact more actively with serum proteins due to their larger surface area.

To know whether the optimized DL-G3-based lipoplex can be used for another type of cells, we further examined transfection of HepG2 cells, which are frequently used for the evaluation of transfection activity for various types of gene vectors. We found that the cells after treatment with this lipoplex in the absence and in the presence of serum exhibited the luciferase activity of 3.2 ± 0.4 × 10^8 RLU/mg protein and 2.2 ± 0.4 × 10^8 RLU/mg protein (n = 6), respectively. Since CV1 cells treated with this lipoplex in the absence and in the presence of serum showed luciferase activity of about 20 × 10^8 RLU/mg protein and about 3.5 × 10^8 RLU/mg protein, respectively (Figure 4A), this lipoplex seems to be somewhat less effective for HepG2 than CV1 cells. However, the cellular luciferase activity induced by the treatment in the presence of serum was 70% of the luciferase activity induced by the treatment in the absence of serum. This result indicates that this optimized lipoplex could be useful for the transfection of various types of cells in the presence of serum.

Comparison with Various Vectors. To estimate the potential of the DL-G3–DOPE lipoplex as a gene vector, we compared its transfection activity with those of Lipofectamine and SuperFect: both are widely used and commercially available vectors. CV1 cells were treated with the DL-G3–DOPE lipoplexes, the Lipofectamine-plasmid DNA complex, and the SuperFect-plasmid DNA complex in the absence of serum or in the presence of 10% FCS. Figure 6 represents the expression of luciferase in the cells treated with these lipoplexes or complexes. In the absence of serum, DL-G3–DOPE lipoplex induced roughly a two-times-higher level and a six-times-higher level of luciferase expression than Lipofectamine complex and SuperFect complex, respectively. As expected, a decrease in transfection efficiency was shown for all vectors in the presence of serum. Especially, the influence of serum was significant for the Lipofectamine complex. In this case, luciferase expression was reduced to 1/180th of that in the absence of serum. A remarkable decrease in transfection efficiency induced by serum was again evident in transfection with the SuperFect complex, in which the cellular luciferase expression was reduced to 1/50th of that in the absence of serum. A 1/6th-fold reduction was apparent in the case of the DL-G3–DOPE lipoplex-mediated transfection in the presence of serum. However, this lipoplex displayed a reduction with much less extent of magnitude than other complexes. As a result, this lipoplex achieved 48–64-times higher expression of the introduced gene in CV1 cells than these widely used vectors under experimental conditions, suggesting its usefulness as a vector for use in the presence of serum.

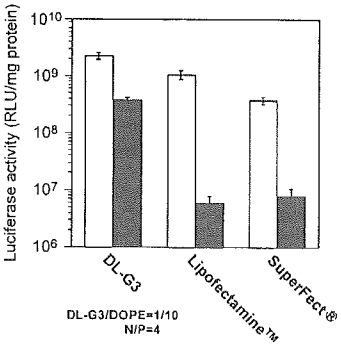

Figure 6. Comparison of transfection activity of DL-G3–DOPE lipoplex with Lipofectamine and SuperFect reagents. The cells (5 × 10^4) were treated with vectors containing 1μg DNA in the absence (open bars) and presence of 10% FCS (closed bars). The DL-G3–DOPE lipoplex with N/P ratio of 4 and DOPE/DL-G3 ratio of 10 was used. Each bar represents the mean ± SD (n = 3).

CONCLUSION

This work was intended to prepare an efficient vector that can achieve gene transfection of cells in the presence of serum using polyamidoamine dendron-bearing lipid DL-G3 and fusogenic lipid DOPE, by the synergetic action of membrane fusion and the proton sponge effect. Results show that transfection activity of the DL-G3–DOPE lipoplexes was highly dependent on their composition, such as the N/P and DOPE/DL-G3 ratios. However, by adjusting the N/P and DOPE/DL-G3 ratios to 4 and 10, respectively, we obtained a lipoplex that exhibited high transfection activity in the presence and absence of serum. Although the obtained lipoplex showed some extent of reduction of transfection activity in the presence of serum, the lipoplex retained much higher activity than some widely used and commercially available transfection reagents. These results strongly suggest that the DL-G3–DOPE lipoplex is a promising nonviral vector for gene therapy.

ACKNOWLEDGMENT

This work was partly supported by the Grant-in-Aid from Japanese Ministry of Education, Culture, Sports, Science, and Technology (16300159). T. Takahashi thanks the Research Fellowships of the Japan Society for the Promotion of Science for Young Scientists.

LITERATURE CITED

(1) Brown, M. D., Schätzlein, A. G., and Uchegbu, I. F. (2001) Gene delivery with synthetic (non viral) carriers. *Int. J. Pharm. 229*, 1–21.
(2) Behr, J. P. (1993) Synthetic gene-transfer vectors. *Acc. Chem. Res. 26*, 274–278.
(3) Zou, S. M., Behr, J. P., Goula, D., and Demeneix, B. (2000) Gene delivery with polyethylenimine. *Gene Therapy: Therapeutic mechanisms and strategies* (Templeton, N. S., Lasic, D. D., Eds.) pp 131–139, Marcel Dekker, New York.
(4) Godbey, W. T., Wu, K. K., and Mikos, A. G. (1999) Poly(ethylenimine) and its role in gene delivery. *J. Controlled Release 60*, 149–160.
(5) Kubasiak, L. A., and Tomalia, D. A. (2004) Cationic dendrimers as gene transfection vectors: dendri- poly(amidoam-

ines) and dendri- poly(propyleneimines). *Polymeric Gene Delivery: Principles and Applications* (Amiji, M. M., Ed.) pp 133−157, Chapter 9, CRC Press, Boca Raton.
(6) Boussif, O., Lezoualc'h, F., Zanta, M. A., Mergny, M. D., Scherman, D., Demeneix, B., and Behr, J. P. (1995) A versatile vector for gene and oligonucleotide transfer into cells in culture and in vivo: Polyethylenimine. *Proc. Natl. Acad. Sci. U.S.A. 92*, 7297−7301.
(7) Takahashi, T., Kono, K., Itoh, T., Emi, N., and Takagishi, T. (2003) Synthesis of novel cationic lipids having polyamidoamine dendrons and their transfection activity. *Bioconjugate Chem. 14*, 764−773.
(8) Farhood, H., Bottega, R., Epand, R. M., and Huang, L. (1992) Effect of cationic cholesterol derivatives on gene-transfer and protein-kinase-C activity. *Biochim. Biophys. Acta 1111*, 239−246.
(9) Wilke, M., Bijma, A., Timmers-Reker, A. J., Scholte, B. J., and Sinaasapp, A. (1997) Complementation of the genetic defect in Gunn rat hepatocytes in vitro by highly efficient gene transfer with cationic liposomes. *Gene Ther. 4*, 1305−1312.
(10) Escriou, V., Ciolina, C., Lacroix, F., Byk, G., Scherman, D., and Wils, P. (1998) Cationic lipid-mediated gene transfer: effect of serum on cellular uptake and intracellular fate of lipopolyamine/DNA complexes. *Biochim. Biophys. Acta 1368*, 276−288.
(11) Turek, J., Dubertret, C., Jaslin, G., Antonakis, K., Scherman, D., and Pitard, B. (2000) Formulations which increase the size of lipoplexes prevent serum-associated inhibition of transfection. *J. Gene Med. 2*, 32−40.
(12) Yang, J. P., and Huang, L. (1997) Overcoming the inhibitory effect of serum on lipofection by increasing the charge ratio of cationic liposome to DNA. *Gene Ther. 4*, 950−960.
(13) Yang, J. P., and Huang, L. (1998) Time-dependent maturation of cationic liposome-DNA complex for serum resistance. *Gene Ther. 5*, 380−387.
(14) Li, S., Tseng, W. C., Stolz, D. B., Wu, S. P., Watkins, S. C., and Huang, L. (1999) Dynamic changes in the characteristics of cationic lipidic vectors after exposure to mouse serum: implications for intravenous lipofection. *Gene Ther. 6*, 585−594.
(15) Crook, K., Stevenson, B. J., Dubouchet, M., and Porteous, D. J. (1998) Inclusion of cholesterol in DOTAP transfection complexes increases the delivery of DNA to cells in vitro in the presence of serum. *Gene. Ther. 5*, 137−143.
(16) Tranchant, I., Thompson, B., Nicolazzi, C., Mignet, N., and Scherman, D. (2004) Physicochemical optimisation of plasmid delivery by cationic lipids. *J. Gene Med. 6*, S24−S35.
(17) Kono, K., Torikoshi, Y., Mitsutomi, M., Itoh, T., Emi, N., Yanagie, H., and Takagishi, T. (2001) Novel gene delivery systems: complexes of fusogenic polymer-modified liposomes and lipoplexes. *Gene. Ther. 8*, 5−12.
(18) Kursa, M., Walker, G. F., Roessler, V., Ogris, M., Roedl, W., Kircheis, R., and Wagner, E. (2003) Novel shielded transferrin-polyethylene glycol-polyethylenimine/DNA complexes for systemic tumor-targeted gene transfer. *Bioconjugate Chem. 14*, 222−231.
(19) Kyriakides, T. R., Cheung, C. Y., Murthy, N., Bornstein, P., Stayton, P. S., and Hoffman, A. S. (2002) pH-Sensitive polymers that enhance intracellular drug delivery in vivo. *J. Controlled Release 78*, 295−303.
(20) Kichler, A., Mechtler, K., Behr, J. P., and Wagner, E. (1997) Influence of membrane-active peptides on lipospermine/DNA complex mediated gene transfer. *Bioconjugate Chem. 8*, 213−221.
(21) Finsinger, D., Remy, J. S., Erbacher, P., Koch, C., and Plank, C. (2000) Protective copolymers for nonviral gene vectors: synthesis, vector characterization and application in gene delivery. *Gene Ther. 7*, 1183−1192.
(22) Farhood, H., Serbina, N., and Huang, L. (1995) The role of dioleoyl phosphatidylethanolamine in cationic liposome mediated gene transfer. *Biochim. Biophys. Acta 1235*, 289−295.
(23) Hui, S. W., Langner, M., Zhao, Y. L., Ross, P., Hurley, E., and Chan, K. (1996) The role of helper lipids in cationic liposome-mediated gene transfer. *Biophys. J. 71*, 590−599.
(24) Zelphati, O., and Szoka, F. C. (1996) Mechanism of oligonucleotide release from cationic liposomes. *Proc. Natl. Acad. Sci. U.S.A. 93*, 11493−11498.
(25) Moret, I., Peris, J. E., Guillem, V. M., Benet, M., Revert, F., Dasi, F., Crespo, A., and Alino, S. F. (2001) Stability of PEI-DNA and DOTAP-DNA complexes: effect of alkaline pH, heparin and serum. *J. Controlled Release 76*, 169−181.
(26) Casu, B. (1985) Structure and biological activity of heparin. *Adv. Carbohydr. Chem. Biochem. 43*, 51−134.
(27) Rabenstein, D. L. (2002) Heparin and heparan sulfate: structure and function. *Nat. Prod. Rep. 19*, 312−331.

BC050012F

THE JOURNAL OF BIOLOGICAL CHEMISTRY
Vol. 280, No. 15, Issue of April 15, pp. 14716–14722, 2005
Printed in U.S.A.

Phosphorylation of Ser-446 Determines Stability of MKP-7*

Received for publication, January 6, 2005
Published, JBC Papers in Press, February 2, 2005, DOI 10.1074/jbc.M500200200

Chiaki Katagiri‡, Kouhei Masuda‡, Takeshi Urano§, Katsumi Yamashita¶, Yoshio Araki, Kunimi Kikuchi‡, and Hiroshi Shima‡‖**

*From the ‡Division of Biochemical Oncology and Immunology, Institute for Genetic Medicine, Hokkaido University, Kita-15, Nishi-7, Kita-ku, Sapporo 060-0815, Japan, the §Department of Biochemistry II, Nagoya University Graduate School of Medicine, 65 Tsurumai, Showa-ku, Nagoya 466-0065, Japan, the ¶Division of Life Science, Graduate School of Natural Science and Technology, Kanazawa University, Kakuma-machi, Kanazawa, 920-1192, Japan, and the **Division of Bioscience, Graduate School of Environmental Earth Science, Hokkaido University, Kita-10, Nishi-5, Kita-ku, Sapporo 060-0810, Japan*

MAPK cascades can be negatively regulated by members of the MAPK phosphatase (MKP) family. However, how MKP activity is regulated is not well characterized. MKP-7, a JNK-specific phosphatase, possesses a unique COOH-terminal stretch (CTS) in addition to domains conserved among MKP family members. The CTS contains several motifs such as a nuclear localization signal, a nuclear export signal, PEST sequences, and a serine residue (Ser-446) that can be phosphorylated by activated ERK, suggesting an important regulatory role(s). ^{35}S-pulse labeling experiments indicate that the half-life of MKP-7 is 1.5 h, a period significantly elongated by deleting the CTS. We also show that overexpressed MKP-7 is polyubiquitinated when co-expressed with ubiquitin and that proteasome inhibitors markedly inhibit MKP-7 degradation. We also determined that MKP-7 phosphorylated at Ser-446 has a longer half-life than unphosphorylated form of the wild type protein, as does a phospho-mimic mutant of MKP-7. These results indicate that activation of the ERK pathway strongly blocks JNK activation through stabilization of MKP-7 mediated by phosphorylation.

In all eukaryotic organisms mitogen-activated protein (MAP)[1] kinase modules are involved in signal transduction of numerous cellular responses including proliferation, differentiation, and apoptosis (1, 2). Three subfamilies of MAP kinases (MAPKs) have been well characterized: ERKs (extracellular signal-regulated protein kinases), JNKs (c-Jun NH_2-terminal kinases), and the p38 MAPK kinases. It is well established that ERK1/2 are typically stimulated by growth-related stimuli, while JNK and p38 are primarily activated by stress-related signals such as heat and osmotic shock, UV irradiation, and inflammatory cytokines. MAPK pathways are regulated at multiple levels to ensure the specificity, timing, and strength of their activity. One critical aspect of this regulation is reversible phosphorylation of MAPKs.

Negative regulation of MAPKs is achieved by dual dephosphorylation of the TXY motif by phosphatases. As *in vivo* candidates for negative regulators, the MAPK phosphatases (MKPs), a family of dual specificity protein phosphatases, have been identified (3). MKPs are primarily composed of two domains, a rhodanese-like domain and a dual specificity phosphatase catalytic domain (4). In mammals 10 genes encoding MKPs differing in substrate specificity and subcellular localization have been reported. According to phylogenetic analysis and gene structure, MKPs can be classified into four groups (5–7). Group I contains the nuclear MKPs: MKP-1/DUSP1, PAC1/DUSP2, MKP-2/DUSP4, and hVH-3/DUSP5, all of which target the three primary MAPKs, ERK, JNK, and p38. Group II includes cytoplasmic MKPs that mainly target ERK, namely, MKP-3/DUSP6, PYST2/DUSP7, and MKP-4/DUSP9. Group III contains MKP-5/DUSP10, which exhibits a unique NH_2-terminal domain in addition to the MKP common structure. MKP-5, which is both nuclear and cytoplasmic, dephosphorylates JNK and p38. Group IV consists of the nuclear and cytoplasmic MKPs, hVH5/DUSP8, and MKP-7/DUSP16. These proteins exhibit a unique COOH-terminal sequence of about 300 amino acid residues in addition to the common MKP structure (8, 9).

We previously showed that MKP-7 shuttles between the nucleus and the cytoplasm and suppresses activation of MAP kinases in COS-7 cells in the order of selectivity JNK $\gg$ p38 $>$ ERK. Using several mutant proteins, we found that a long COOH-terminal stretch (CTS) contains a functional nuclear export signal and a nuclear localization signal, both of which enable MKP-7 to shuttle between the nucleus and the cytoplasm, and that the CTS determines JNK preference for MKP-7 by masking MKP-7 activity toward p38 (8). Recently we found that the CTS domain is bound by ERK and that Ser-446 in the CTS is phosphorylated by ERK depending on several external stimuli (10). These data strongly suggest that the CTS plays important regulatory role(s) in cells.

Although very few studies address their post-translational regulation, it is known that some MKP/dual specificity phosphatases can be phosphorylated and/or polyubiquitinated. MKP-1 is phosphorylated by ERK on two COOH-terminal serine residues, Ser-359 and Ser-364, which does not directly affect phosphatase activity but results in stabilization of the protein due to reduced degradation by the ubiquitin-directed proteasome complex (11). VH-1-related phosphatase (VHR) has also been reported to be phosphorylated on Tyr-138 by ZAP-70, resulting in translocation of VHR to the immune synapse (12). So far some MKPs have been reported to be phosphorylated.

* This work was supported in part by Grants-in-aid for Scientific Research (B) provided by Japan Society for the Promotion on Science, and a Grant-in aid for Scientific Research on Priority Area (A) provided by the Ministry of Education, Culture, Sports, Science, and Technology of Japan. The costs of publication of this article were defrayed in part by the payment of page charges. This article must therefore be hereby marked "*advertisement*" in accordance with 18 U.S.C. Section 1734 solely to indicate this fact.

‖ To whom correspondence should be addressed. Tel.: 81-11-706-5536; Fax: 81-11-706-7541; E-mail: hshima@igm.hokudai.ac.jp.

[1] The abbreviations used are: MAP, mitogen-activated protein; MAPK, MAP kinase; ERK, extracellular signal-regulated kinase; JNK, c-Jun NH_2-terminal kinase; MEK, MAP kinase/ERK kinase; MKP, MAP kinase phosphatase; HA, hemagglutinin; PMA, 12-*O*-tetradecanoylphorbol-13-acetate; CTS, COOH-terminal stretch, DAPI, 4′,6-diamidino-2-phenylindole; WT, wild type.

MKP-1 is phosphorylated by ERK1/2 *in vivo* as well as *in vitro*, which inhibits protein degradation. hVH-5 is phosphorylated in response to PMA treatment, but the physiological consequences of such modification are not known (13). *Xenopus* CL100 (XCL100), a homologue of human MKP-1, is phosphorylated by ERK in a cell cycle-dependent manner (14). In the case of XCL100, serine residue(s) are phosphorylated during the G_2 phase, and serine and threonine residues are phosphorylated during M phase. Experiments with proteasome inhibitors demonstrate that not only MKP-1 but MKP-2 degradation is mediated via the ubiquitin-proteasome pathway (15).

Recently we found that the CTS of MKP-7 is bound by ERK and that Ser-446 in the CTS is phosphorylated by ERK in response to several external stimuli (10). Since MKP-7 is a JNK phosphatase, it is important to analyze physiological significance of phosphorylation of MKP-7 by ERK. Such analysis could explain how MKP-7 links ERK activity to stress kinase activations. The CTS in MKP-7 contains two PEST sequences (regions abundant in proline, glutamate, serine, and threonine residues) (8), which are found in many rapidly degraded proteins and have been suggested to signal proteolytic degradation (16, 17). The presence of such sequences predicts that MKP-7 could be a relatively unstable protein (8). We and others (10, 18) previously showed that expression levels in cells of COOH-terminally truncated MKP-7 and mouse MKP-M, a homologous to the human MKP-7, are higher than that of the wild type protein, supporting such an idea. In the present study, we determine the stability of MKP-7 and identify sequences mediating protein degradation. We also analyze the effect of Ser-446 phosphorylation on MKP-7 stability.

EXPERIMENTAL PROCEDURES

Plasmid Construction—Mammalian expression vectors, pFLAG-MKP-7, pFLAG-MKP-7-(1–370), -(1–568), and -(1–604), and -S446A have been described previously (8, 10). Point mutations of pFLAG-MKP-7S446A and S446D were generated by site-directed mutagenesis using the QuikChange site-directed mutagenesis system (Stratagene). pFLAG-MKP-7-(1–435), -(1–511), -(162–665), -(371–665), -(371–665)-S446A, -371–665)S446D, -(390–665), -(436–665), -436–665)S446A, -Δ406–540, -ΔP1 (deletion from 332–353), and -ΔP2 (deletion from 441–462) were constructed by PCR. To construct pFLAG-MKP-2, pFLAG-MKP-3, and pFLAG-MKP-5, the coding region of human MKP-2, MKP-3, and MKP-5 were amplified by reverse transcription-PCR and subcloned into the pFLAG-CMV2 vector (Sigma). pCI-neo-T7-ubiquitin and pCI-neo-HA-ubiquitin were kind gifts of Dr. Yokosawa (19).

Cell Culture and DNA Transfection—COS-7 and HeLa cells were maintained in Dulbecco's modified Eagle's medium containing 10% fetal bovine serum at 37 °C under 5% CO_2. Cells were transfected with various expression vectors using the FuGene-6 transfection reagent (Roche Diagnostics Inc.) according to the manufacturer's recommendation.

^{35}S Pulse-Chase Analysis—At 32 h after DNA transfection, COS-7 cells were cultured in the presence of a Expre^{35}S^{35}S protein labeling mix (PerkinElmer Life Sciences) for 1 h. The radioactive medium was removed, and cells were chased with non-radioactive medium. At the indicated times, cells were lysed with immunoprecipitation buffer containing 50 mM Tris-HCl (pH 7.5), 150 mM NaCl, 2 mM EDTA, 10% glycerol, 1% Triton X-100, 1 mM phenylmethylsulfonyl fluoride, 10 μg/ml leupeptin, and 10 μg/ml aprotinin. Cell lysates were centrifuged at 20,000 × *g* for 10 min, and the resulting supernatants were used as cell extracts. Each sample was immunoprecipitated with 2 μg of mouse anti-FLAG M2 antibody (Sigma) and 15 μl of protein G-Sepharose 4 fast flow (Amersham Biosciences). Immunoprecipitated proteins were separated by SDS-PAGE on a 10% gel. The intensity of bands of FLAG-MKP-7 and mutant proteins was quantified using an FLA-3000 imaging system (Fujifilm, Tokyo, Japan).

Immunoblot Analysis of Cells Treated with Cycloheximide and Proteasome Inhibitors—Eighteen hours after DNA transfection, COS-7 cells (2×10^5/35-mm-diameter plate) were starved for 14 h and treated with 10 μg/ml cycloheximide for the indicated times. To determine the effect of proteasome-mediated proteolysis, 20 μM MG115 (Peptide Institute, Osaka, Japan), 20 μM MG132 (Peptide Institute), or Me_2SO as a vehicle was added 2 h before cycloheximide treatment. For immunoblot analysis, cells were lysed in MAPK lysis buffer as described previously (10). Cell lysates were subjected to immunoblot with anti-FLAG M2 or anti-actin (Sigma) antibody.

Ubiquitination Assay—COS-7 cells (4×10^5/60-mm-diameter plate) were transfected with 2.4 μg of pFLAG-MKP-7 together with 0.4 μg each of pCI-neo-T7-ubiquitin and pCI-neo-HA-ubiquitin. Eighteen hours after transfection, cells were starved for 12 h and then treated with 20 μM MG132 for 6 h. The cells were lysed in MAPK buffer and subjected to immunoprecipitation using 3 μg of anti-FLAG M2 monoclonal antibody and 15 μl of protein G-Sepharose 4 fast flow. Immunoprecipitated proteins were separated on a 10% gel and subjected to immunoblot using anti-T7 monoclonal antibody (Novagen) or anti-FLAG polyclonal antibody (8).

Cell Staining—Immunohistochemical analyses were performed as described (8). To detect FLAG-tagged proteins immunofluorescence was performed using anti-FLAG rabbit antibody with AlexaFluor 488-conjugataed anti-rabbit IgG secondary antibody (Invitrogen) or AlexaFluor 546-conjugated anti-rabbit IgG secondary antibody (Invitrogen). To detect phospho-Ser-446 of MKP-7 immunofluorescence was undertaken using anti-phospho-Ser-446 antibody with AlexaFluor 546-conjugated goat anti-mouse IgG secondary antibody (Invitrogen) or AlexaFluor 488-conjugataed anti-mouse IgG secondary antibody (Invitrogen). Nuclei were detected by staining with 1 μg/ml 4–6-diamidino-2-phenylindole (DAPI). Fluorescence was visualized under a fluorescence confocal microscope (Olympus). Anti-phospho-Ser-446 monoclonal antibody was developed against a phosphopeptide NKLCQFpSPVQEC as described previously (20).

RESULTS

MKP-7 Is an Unstable Protein in COS-7 Cells—To determine whether MKP-7 is rapidly degraded, pulse-chase experiments were performed. COS-7 cells transiently transfected with pFLAG-MKP-7 were pulse-labeled with [^{35}S]methionine for 1 h and chased with non-radioactive medium up to 4 h. Radiolabeled FLAG-MKPs were precipitated with an anti-FLAG antibody at 0-, 1-, 2-, and 4-h chase time points and subjected to autoradiography (Fig. 1, *insets*). The half-life of MKP-7 was shown to be 1.5 h (Fig. 1*a*). Under the same experimental conditions, half-lives of MKP-2, MKP-3, and MKP-5, which are representative of groups I, II, and III, respectively, were analyzed. The half-life of MKP-2, known to be a short-lived protein due to proteasome-dependent degradation (15), was shown to be 1.2 h (Fig. 1*b*). The half-lives of MKP-3 and MKP-5 were both 4 h (Fig. 1*c* and *d*). These data indicate that like MKP-2, but unlike MKP-3 and MKP-5, MKP-7 is a highly unstable protein.

MKP-7 Is Degraded by a Ubiquitin-dependent Pathway—To determine whether the rapid turnover of MKP-7 is due to proteasomal activity, we analyzed the effect of two proteasome inhibitors, MG115 and MG132, on degradation of MKP-7 (Fig. 2*A*). Immunoblot analysis showed that in the absence of inhibitors, levels of FLAG-MKP-7 were rapidly decreased in the presence of cycloheximide, an inhibitor of *de novo* protein synthesis. This reduction was completely inhibited by treatment of COS-7 cells with MG115 or MG132. Under these conditions, the amounts of actin were constant. These results suggest that MKP-7 is degraded by the proteasome. An important component of proteasome-mediated degradation is the proper targeting of the protein to be degraded by the ubiquitin conjugation complex (21). This process results in the attachment of multiple ubiquitin chains to the target protein. To determine whether MKP-7 was ubiquitinated, we transiently overexpressed FLAG-MKP-7 in COS-7 cells with or without T7- and HA-ubiquitin. Proteins were similarly ubiquitinated in lysates from cells with or without co-expressed FLAG-MKP-7 (Fig. 2*B*, *right*). FLAG-MKP-7 was purified from the FLAG-MKP-7 containing cell extracts using anti-FLAG-Sepharose (Fig. 2*B*, *left*). A high molecular weight smear, characteristic of polyubiquitination, was observed in lysates from cells in which MKP-7 and ubiquitin were co-expressed, demonstrating that MKP-7 is degraded by the ubiquitin/proteosomal pathway (Fig. 2*B*, *left*).

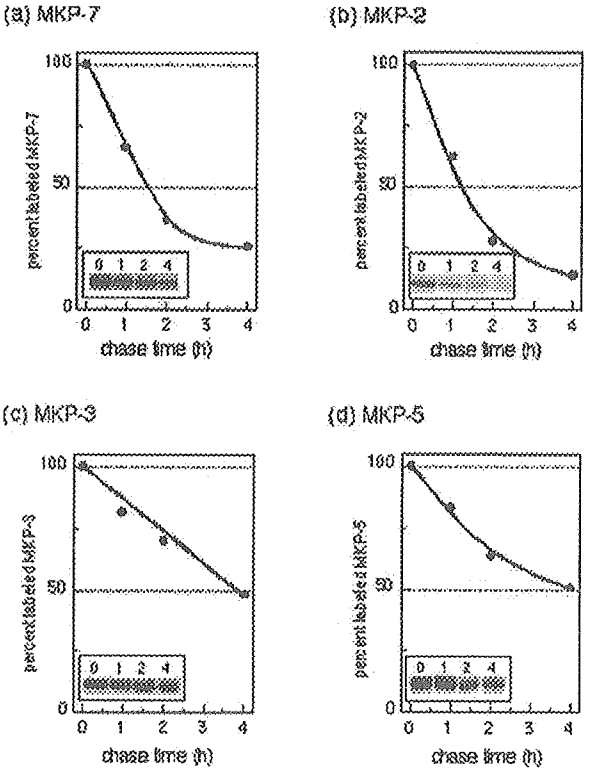

FIG. 1. **Comparison of stability of MKP-7 and other MKPs including MKP-2, MKP-3, and MKP-5.** COS-7 cells (2×10^5/35-mm-diameter plate) were transfected with 1.2 μg of pFLAG-MKP-7 (*a*), pFLAG-MKP-2 (*b*), pFLAG-MKP-3 (*c*), or pFLAG-MKP-5 (*d*). After 32 h in culture, cells were pulsed with [^{35}S]methionine for 1 h and chased for the indicated times. Cells were lysed, and samples were subjected to immunoprecipitation with anti-FLAG antibody followed by SDS-PAGE. The levels of [^{35}S]methionine-labeled pFLAG-MKPs were monitored by autoradiography as shown in the *insets*. The graph shows the relative intensity of [^{35}S]methionine labeled MKPs. Intensities relative to that seen in cells without chase are presented. Data shown are the means from three independent experiments.

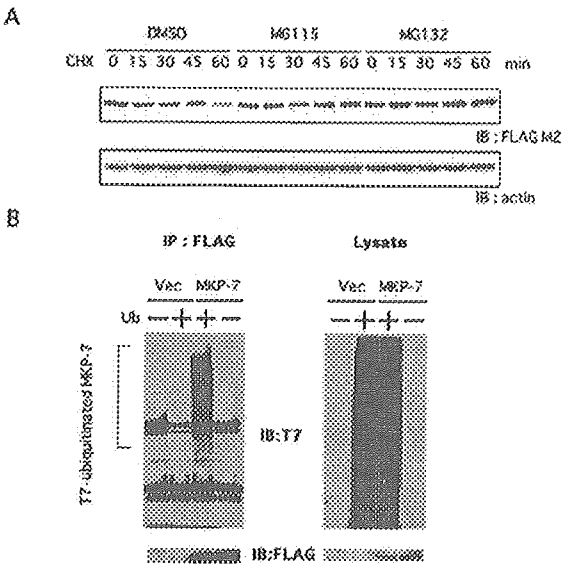

FIG. 2. **MKP-7 is degraded by an ubiquitin-dependent pathway.** *A*, COS-7 cells (2×10^5/35-mm-diameter plate) were transfected with 1.2 μg of pFLAG-MKP-7. After 30 h of culture, cells were cultured without or with either 20 μM MG115 or MG132 for 2 h. Cells were then treated with 10 μg/ml cycloheximide (*CHX*) for the indicated times, and levels of FLAG-MKP-7 and actin were monitored by immunoblot (*IB*) with anti-FLAG M2 antibody (*upper panel*) or anti-actin antibody (*lower panel*). *DMSO*, dimethyl sulfoxide. *B*, COS-7 cells (4×10^5/60-mm-diameter plate) were transfected with 2.4 μg of pFLAG-MKP-7 with or without 0.4 μg each of pCI-neo-T7-ubiquitin and pCI-neo-HA-ubiquitin. Eighteen hours after transfection, cells were starved for 12 h and treated with 20 μM MG132 for 6 h. An immunoprecipitation (*IP*)/immunoblot (*IB*) of the cell lysate was done using anti-FLAG M2 antibody for the immunoprecipitation and either anti-T7 antibody (*left, upper panel*) or anti-FLAG polyclonal antibody (*left, lower panel*) for the immunoblot. Levels of ubiquitinated proteins and FLAG-MKP-7 in cell extracts were monitored by immunoblot with anti-T7 antibody (*right, upper panel*) or anti-FLAG polyclonal antibody (*right, lower panel*). *Vec*, vector; *Ub*, ubiquitin.

Deletion of the COOH-terminal Region Affects Stability of MKP-7 but Deletion of the PEST Sequences Does Not—To determine sequences required for ubiquitin-proteasome dependent degradation of MKP-7, we prepared constructs of two deletion mutants, MKP-7-(162–665) and MKP-7-(1–370). Pulse-chase experiments showed that the degradation rate of MKP-7-(162–665) was similar to that of the wild type protein, while MKP-7-(1–370) was stable until 4 h (Fig. 3*A*), suggesting that the stability of MKP-7 is determined primarily by amino acid residues between 371 and 665. Previously we reported the presence of two PEST sequences, PEST1 (332–353, PEST score = 7.16) and PEST2 (441–462, PEST score = 5.16). To clarify whether the PEST sequences of MKP-7 are required for its degradation, we prepared constructs encoding mutant proteins, MKP-7ΔP1 and -ΔP2, which lack PEST1 and PEST2, respectively. Interestingly, the half-lives of MKP-7ΔP1 and -ΔP2 were similar to that of the wild type protein (Fig. 3*B*), indicating that instability of MKP-7 is not conferred by the PEST regions.

Identification of Sequences in the CTS Required for Degradation of MKP-7—To determine which sequences in the CTS play a role in stability, expression vectors encoding COOH-terminal deletion mutant proteins, MKP-7-(1–604), -(1–568), -(1–511), -(1–435), and -Δ406–540 were constructed (Fig. 4*A*). Using pulse-chase analysis, the half-lives of wild type and mutant proteins were calculated (Fig. 4*B*). The half-life of MKP-7-(1–604), which was 1.7 h, was similar to that of the wild type protein. However, the half-lives of MKP-7-(1–568) and MKP-7-(1–511) were 5.0 and 4.8 h, respectively, indicating that amino acid residues 569–604 are involved in protein degradation. By contrast, degradation of MKP-7-(1–435) was not observed until 4 h. The observation that PEST2 is equivalent to amino acid residues 441–462 indicates that it is not involved in degradation (Fig. 3*B*) and suggests rather that amino acid residues 463–511 are involved in protein degradation. We designated residues 463–511 and 569–604 as regions 1 and 2, respectively. The half-life of MKP-7Δ406–540, which contains region 2 but lacks region 1, was shown to be 3.5 h. These data indicated that the CTS, in particular regions 1 and 2, are involved in degradation of MKP-7.

Detection of Upward Mobility Shift of the CTS—To examine the relationship between phosphorylation at Ser-446 of MKP-7 and its degradation through the CTS, we prepared expression vectors of CTS fragments including Ser-446. COS-7 cells, transfected with pFLAG-MKP-7-(371–665), -(390–665), or -(436–665) (Fig. 5), were labeled with [^{35}S]methionine and chased. We found that ^{35}S-labeled MKP-7-(371–665) and MKP-7-(390–665) were detected as doublets, while ^{35}S-labeled MKP-7-(436–665) was seen as a single band by autoradiography (Fig. 5, *insets*). The half-lives of the lower bands of pFLAG-MKP-7-(371–665) and MKP-7-(390–665) were 1.2 and 1.5 h, respectively, which are equivalent to that of the wild type MKP-7